INVESTIGATING THE ACCURACY AND USE OF DIGITAL

ORTHO-IMAGES (DOIs)

By

George A. Dordah BSc (Hons) Geomatic Engineering

KNUST

A Thesis Submitted to the Department of Geomatic Engineering,

Kwame Nkrumah University of Science and Technology

In partial fulfillment of the requirements for the Degree

Of

Master of Science

Faculty of Civil and Geomatic Engineering

College of Engineering

February 2009

DECLARATION

I hereby declare that this submission is my own work towards the award of Master of Science and that, to the best of my knowledge, contains no material previously published by another person nor material which has been accepted for the award of any other degree of the University, except where due acknowledgement has been made in the text.
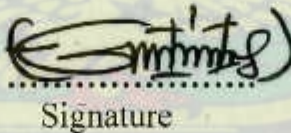
George A. Dordah
....
Name of Student

....
Signature

02 - 10 - 2009
....
Date

Certified by:

Dr. Eric K. Forkuo
....
Name of Supervisor

....
Signature

02-10-2009
....
Date

Certified by:

Dr. Eric K. Forkuo
....
Name of Head of Department

....
Signature

02-/0-2009
....
Date

Abstract

As the field of photogrammetry moves to the digital domain, it is being effectively used for the production of Digital orthoimages (DOIs). DOIs have numerous advantages including its use as an excellent base layer for geographic information systems (GIS). However, a significant segment of the user community is concerned about product accuracy of DOIs. The objectives of this research include investigating the significance of the effect of varying number of Ground Controls Points (GCPs), varying grid intervals of digital elevation model (DEM) and varying scale corresponding to different pixel sizes on the planimetric accuracy of DOIs and the effect of accuracy on use.

The main findings of the research revealed that a variation in the number of GCP had significant effect on the planimetric accuracy of the final DOI produced compared with the variation in DEM grid interval and variation in scale. In addition, it was clear that DOIs can be used for the purposes of most small and large scale maps. However they cannot be used at scales beyond the allowable magnification of the source scale.

Keywords: *Digital, Accuracy, Analysis, Production, Photogrammetry, Aerial triangulation, Digital Terrain Model, Orthoimages, orthorectification*

I
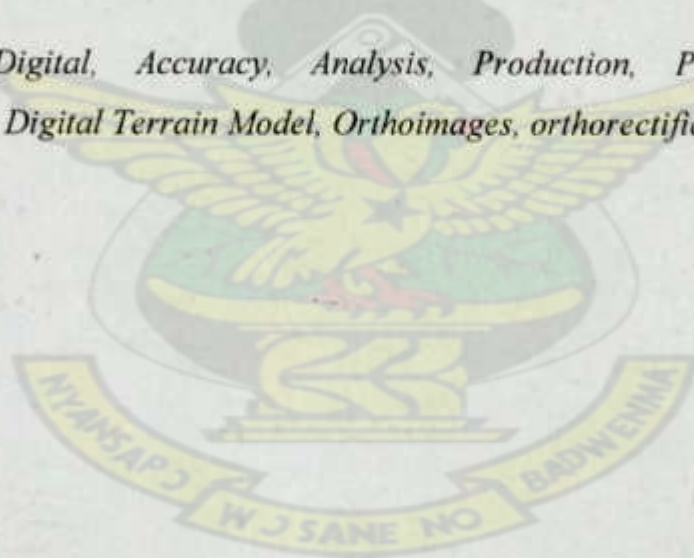
Dedication

This Thesis is dedicated to my late father Mr. Alexander Pious Dordah, my wonderful family and all my friends.

Acknowledgements

Table of Contents

CHAPTER 3: MATERIALS AND METHODS

CHAPTER 4: RESULTS AND ANALYSIS

CHAPTER 5: CONCLUSIONS AND RECOMMENDATIONS

List of Figures

List of Tables

VIII

List of abbreviations

AO	Absolute Orientation
ASP	American Society of Photogrammetry
AT	Aerial Triangulation
DOI	Digital Orthoimage
DP	Digital Photogrammetry
DPS	Digital Photogrammetric system
DPW	Digital Photogrammetric Workstation
DEM	Digital Elevation Model
EO	Exterior Orientation
FGDC	Federal Geographic Data Committee
GCP	Ground Control Point
GDPS	Differential Global Positioning System
GRN	Ghana Reference Network
GIS	Geographic Information System
GPS	Global Positioning System
GSD	Ground Sample Distance
IO	Interior Orientation
IMU	Inertial Measurement Unit
INS	Inertial Navigation System
ISPRS	International Society for Photogrammetry and Remote Sensing
LAP	Land Administration Project
MSE	Mean Square Error

NMAS	National Map Accuracy Standards
NSSDA	National Standard for Spatial Data Accuracy
OI	Orthoimages
Osi	Ordinance Survey Ireland
PaMAGIC	Pennsylvania Mapping and Geographic Information Consortium
RMS	Root Mean Squares
RMSE	Root Mean Square Error
RO	Relative Orientation
SAR	Synthetic Aperture Radar
TIN	Triangulated Irregular Network
USGS	United States Geological Survey

CHAPTER ONE

INTRODUCTION

1.1 Background

Photogrammetry aims at the production of maps from aerial photographs which are normally captured with the use of a camera on board an air plane. Over the years, photogrammetric techniques based on a stereo pair of vertical aerial photographs have been used for the production of topographic maps and ortho-images (OIs) that have high geometric accuracy (Fletcher, et al., 2003; Moore, 2000).

According to Yamano, et al., (2005) recent advancement in computer technology has made available Digital Photogrammetry (DP), which performs the photogrammetric workflow in a completely digital environment. The move to DP is being driven by the desire to increase production capability through computer automation and to take advantage of new methods, procedures and technologies which lead to the potential of automating photogrammetric production processes efficiently (Kersten, et al., 1999 cited in Helina, 2002) and reducing uncertainty of product accuracy.

A Digital photogrammetric system (DPS) can map digital line vectorgraphs of different scales. The whole resolving scheme of automated aero triangular surveying, image matching techniques and many kinds of high efficiency of the DPS have greatly improved the effectiveness of production (Shen, et al., 2002). In ERDAS (2003), DP is defined as photogrammetry as applied to digital images that are stored and processed on a computer. An example of a DPS is shown in appendix 1.

1

It is reported in ERDAS (2003) that raw aerial photography and satellite imagery have large geometric distortion that is caused by various systematic and non-systematic factors. Photogrammetric modelling is based on collinearity equations thus eliminates these errors most efficiently, and creates the most reliable OI from the raw imagery (e.g., perspective aerial photographs).

Li, et al., (2002) also reported that when di gital ortho-rectification is completed, the central perspective image is transformed into an orthogonal projection which is scale-accurate and can be used as a map. Rossi (2004) as cited in Ayhan, et al., (2006) confirmed that, a digital ortho-image (DOI) displays all the valuable information of a photograph, but unlike aerial photographs, true distances, angles and areas can be measured directly on them.

According to Baltsavias (1995), DOIs provide great advantages in comparison to their analogue counterparts, especially with respect to flexibility, production of derived products and combination with other data sets. It is also reported in Aspinall, et al., (1994) that DOIs have value for supplementing line maps, providing backdrop information to fill the 'blank' areas on maps and therefore facilitating the user their own interpretation of features in the landscape, for example, patterns of land use.

Baltsavias (1995) reported that the production of DOI has become more commonplace due to the development of more powerful computers with sufficient resources, easier acquisition of input data, increased generation of digital data, development of many

2

commercial OI production systems, and new application areas, particularly in connection to geographic information system (GIS) and digital mapping.

DOIs produced with a DPS have unlimited capability and a variety of applications in various areas such as forest management, ecosystem management and environmental planning (Çakır, et al., 2006). In addition, DOIs can be produced with greater speed, lower cost, an effective interface and serve as excellent base data layers to GIS (Li, et al., 2002; Schickler and Thorpe, 1998).

1.2   Problem Statement and Justification

In Ayhan, et al., (2006) it is reported that with the development and advancement in technology, DP is being used widely in almost all areas of mapping. More especially, DOIs which are products of the DPS have become common in their use by lots of private sectors because of their easy interpretability. The ability to produce DOIs provides another source of data for use in GIS (Dowman, et al., 1991; Lenzen and Foresman, 1993 cited in Aspinall, et al., 1994).

DOIs produced from DPS are being applied globally because they have enormous advantages compared with other map production methods. National initiatives on the production of DOI coverage for entire countries are gaining ground (Goebel and Price, 1993; Gunnarsson, 1993; Light, 1993; Skalet, et al., 1992 cited in Aspinall, et al., 1994). To support this submission, Cory and Mcgill (1999) accentuated in the paper "DEM

3

derivation at Ordinance Survey Ireland (Osi)" that regardless of the prevailing debates elsewhere the use of DP at Osi has been successful.

Over the past years, the Survey Department in collaboration with private organizations and other foreign agencies have been addressing the problem of the lack of digital maps in Ghana (Helina, 2002). Though production of DOIs started in Ghana few years ago it has become one of the means by which this problem (lack of digital maps) is being addressed. An example is a project by the Land Administration Project (LAP) which is producing DOIs for most parts of Ghana.

Li, et al., (2002) reported that despite the increasing global use of DOIs, there is still debate in some circles as to the effectiveness of digital over conventional photogrammetry and a significant segment of the user community is still careful about product (e.g., DOIs) accuracy of this new system (DP). Li, et al., (2002) also reported that because the use of DP for map production entails many steps, each imports some errors which can be propagated to the final Product (e.g., DOI) an idea supported by Zhang et al. (2002).

Prior research by Çakır, et al., (2006) shows that the accuracy of the Digital Elevation Model (DEM), clarity and quality of aerial photos, scanning resolution, distribution and accuracy of Ground Control Points (GCPs) and land topography are some of the factors which affect the accuracy of DOIs. An investigation of the accuracy of DOIs is thus imperative in order to analyse and limit error sources and to decrease error propagation so that the end product can constitute a highly geometric reference (Li, et al., 2002; Zhang, et al., 2002).

4

As stated prior in this section, globally considerable investigations have been done on the accuracy implications of some of the factors affecting DOI production. For example, in researches carried out by Çakır, et al., (2006) and Çakır (2006) as cited in Çakır, et al., (2006), it was concluded that accuracy of the final OI created is related to the type of scanner and resolution size used. Ayhan, et al., (2006) also found that when large scale high resolution image, high accuracy DEM and control points are used, high accuracy OI maps will be produced. Li, et al., (2002) thus concluded that, because accuracy assessment of DOIs is a complicated issue, the method of combining theory with practice is suitable.

1.3 Research Objectives

In the midst of the global researches, the main objective of this research is to investigate the effect of some of the steps in DOI production on accuracy and the effect of accuracy on use. More specifically this study would investigate the effect of the number of GCPs supplied, the choice of DEM grid interval used and the scale chosen on the planimetric accuracy of DOIs. The study will also analyse the use of DOIs based on accuracy in relation with scale in order to inform producers to take the necessary measures to produce DOIs of better accuracy so as to enhance reliability.

1.4 Study Area

The research area lies within Latitude 6^0 41' 58" N and Longitude 1^0 33' 17" W, in the Kumasi Metropolis of the Ashanti Region of Ghana. It covers portions of Kentinkrono and Nsenie an area of approximately 2.0kmx1.0km positioned within the overlap area of two stereo pairs of 230mmx230mm taken at a scale of 1:10,000.

5

The study area (Figure 1-1) was chosen based on its proximity to the KNUST campus and the availability of data for the study.
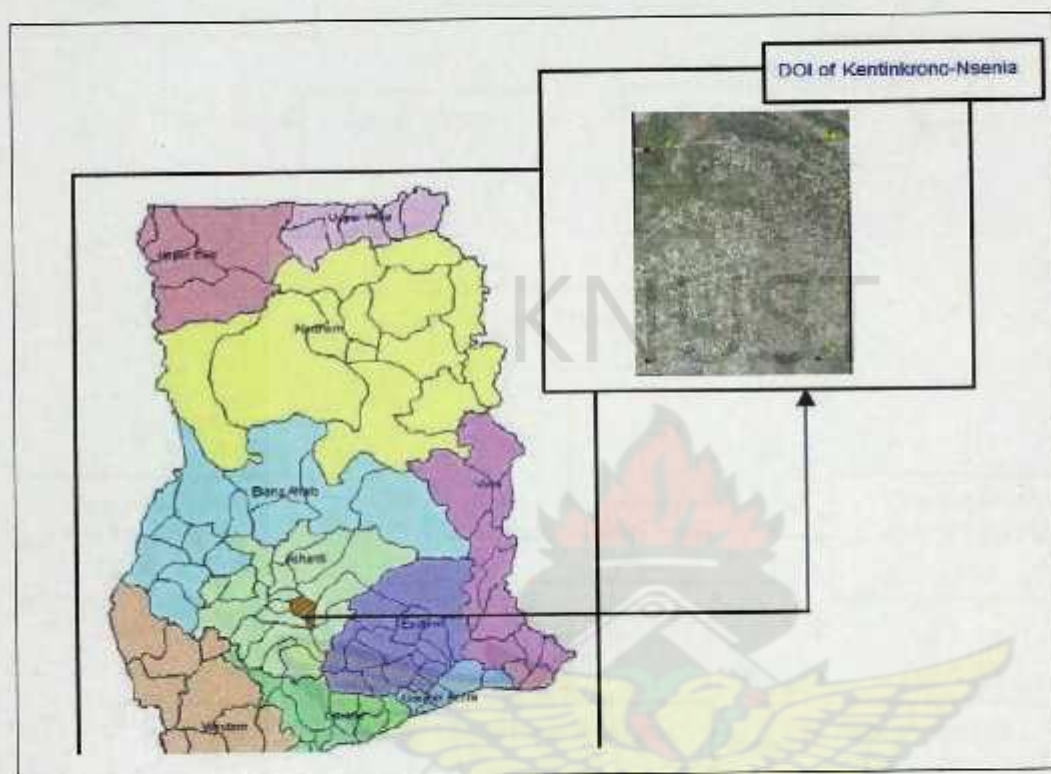
Figure 1-1: A DOI of a portion of kentinkrono-Nsenia in the Ashanti Region

1.5   Structure of Research and Main Approach

This chapter introduced photogrammetry and the advantages of its products, the problem statement, justification and objectives of this research. The chapter two of this thesis reviews literature on the inception of Photogrammetry, the evolutions of the technique and the effect of transition on production, products (e.g., DOI) and accuracy. Chapter three presents the materials and the comprehensive methods used in this study whilst chapter four presents the results obtained and their analysis. Finally chapter five looks at the conclusions and recommendations derived from the main findings of this study.

6

Figure 1-2 is a simplified flow chart of the overview of the main approach of the research.

```
┌─────────────────┐      ┌──────────────────┐      ┌─────────────────┐
│ Reconnaissance  │◄─────│ Data Acquisition │─────►│ Reconnaissance  │
│    (Office)     │      └──────────────────┘      │ (Office & Field)│
└─────────────────┘                                └─────────────────┘
        │                                                   │
        │    ┌──────────────┐      ┌──────────────┐         │
        └───►│ Aerial Photos│      │   GPS GCPs   │◄────────┘
             └──────────────┘      └──────────────┘
                    │                      │
                    │   ┌──────────────┐   │
                    └──►│Data Processing│◄─┘
                        └──────────────┘
                               │
┌─────────────────┐    ┌──────────────────────┐    ┌─────────────────┐
│ Computation of  │◄───│ Generation of DOI    │───►│ Computation of  │
│ RMSE of Edited  │    │      types           │    │ RMSE of other   │
│    DEM DOI      │    └──────────────────────┘    │     DOIs        │
└─────────────────┘                                └─────────────────┘
        │                      │                           │
        ▼                      ▼                           ▼
┌─────────────────┐    ┌──────────────────┐    ┌─────────────────┐
│ Analysis of use │◄───│ Results & Analysis│───►│Accuracy Analysis│
└─────────────────┘    └──────────────────┘    └─────────────────┘
        │                      │                           │
        │   ┌─────────────────────────────────────┐        │
        └──►│  Conclusions & Recommendations       │◄───────┘
            └─────────────────────────────────────┘
```
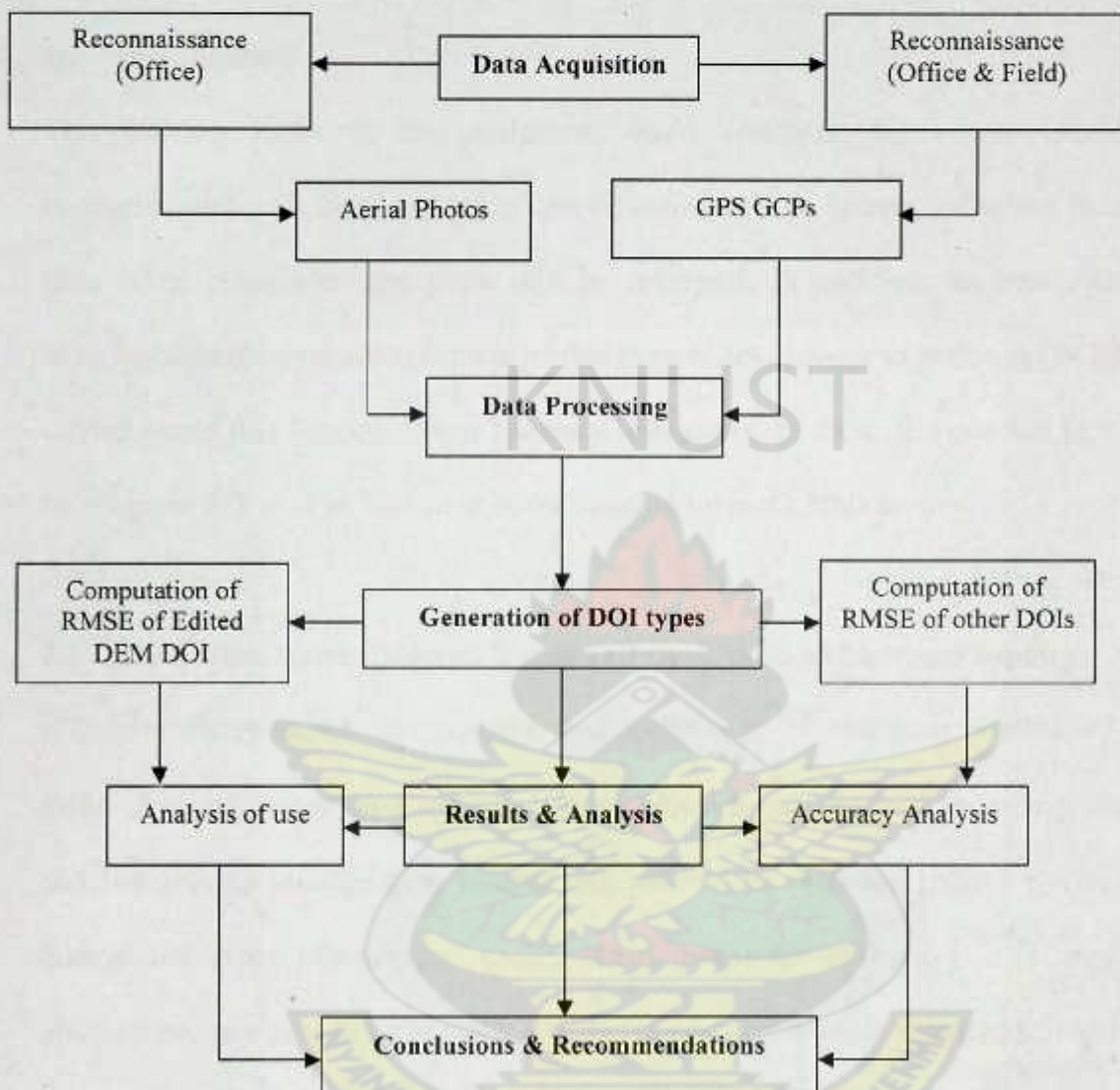
Figure 1-2: Simplified schema of the main research approach

CHAPTER TWO

LITERATURE REVIEW

2.1 Introduction

This Section looks at the definition, basic concepts, types and evolutions of Photogrammetry. A brief history of the inception of this system including changes that have taken place over the years will be reviewed. In addition, an investigation into changes technological advancement of this system has brought to products (DOIs) will be carried out in this Section. Some accuracy implication of these changes and how this can be analysed will also be looked at in the concluding part of this section.

2.2 Definition, basic Concept, Types and Evolutions of Photogrammetry

Photogrammetry is the "art, science, and technology of obtaining reliable information about physical objects and the environment through processes of recording, measuring, and interpreting photographic images and patterns of recorded radiant electromagnetic energy and other phenomena" (ASP, 1980). From the definition, it is implicit that, photogrammetry aids in identifying qualitative and quantitative characteristics of features through the use of aerial photography and also satellites imagery without coming in contact with them.

Photogrammetry can be said to be far range when camera distance setting is indefinite (e.g., photographs taken from airborne vehicles) and close range where finite values are set for the camera distance (e.g., photographs taken from earth-based cameras). It can also be grouped into Aerial (which is mostly far range photogrammetry), and Terrestrial (mostly close range photogrammetry) (Wolf, 1983).

8

The practice of photogrammetry Wolf (1983) stated commenced in 1839 when Louis Daguerre of Paris announced his direct photographic process. It was however invented in 1851 by Laussedat, according to ERDAS (2003) and has continued to develop over the last 140 years.

Konecny (1985) and Konecny (1994) as cited in ERDAS (2003) stated that from around the 1850s, photogrammetry which has extended about fifty years has over time passed through the phases of plane table photogrammetry, analog photogrammetry, analytical photogrammetry and has now entered the phase of DP. The evolving of photogrammetry from the analytical phase to the digital phase has been steady due to intensive research and development of softcopy photogrammetric systems (e.g., Lue, 1996; Miller, et al., 1996; Zhang, et al., 1996 cited in Wang, et al., 2002).

2.3 Effects of changes in technology on Products of Photogrammetry

The traditional and largest application of photogrammetry was in the extraction of topographic information (e.g., topographic maps) from aerial images (ERDAS, 2003). According to Helina (2002), akin to other information-based technologies, the Photogrammetric industry is in steady state of evolution and most up-to-date techniques and instrumentations have been brought into the photogrammetric community. The automation grade in digital systems has improved steadily, especially with the development of automatic aerial triangulation (AT) and automatic DEM extraction (e.g., Ackermann, 1995; Krzystek, et al., 1996; Schenk, 1997; Tang, 1996; Zhang, 1997 cited in Wang, et al., 2002).

9

The high automation in many photogrammetric tasks in DP has resulted in automatic DOI generation (ERDAS, 2003). Thus DOIs are now produced commercially due to the increased availability of more powerful computers, high-resolution metric scanners allowing for accurate digital image creation and image processing tools (Sarjakoski, 1981).

2.4 Processes of DOI Generation

The production of DOIs is preceded by a process called digital ortho-rectification based on interior and exterior orientation (EO) elements of aerial photographs. This process which uses digital image processing and DP techniques for DOI production relies on digital images (Li, et al., 2002). These digital images according to Madani (1996) are the main most significant input for the DOI production process. Other inputs include GCPs and camera calibration parameters (Honkavaara, et al., 1998).

A summary of the DOI production process includes acquiring digital images from sensors or scanned stereo pairs. The digital images then go through the processes of orientations in a DPS after the inputs (stated prior in this section) have been supplied. The next stage is the ortho-rectification process which uses the DEM file created from the X, Y, and Z of the GCPs and the final DOI goes through quality enhancement.

Figure 2-1 is a Schematic diagram of the Work flow of DOI generation.
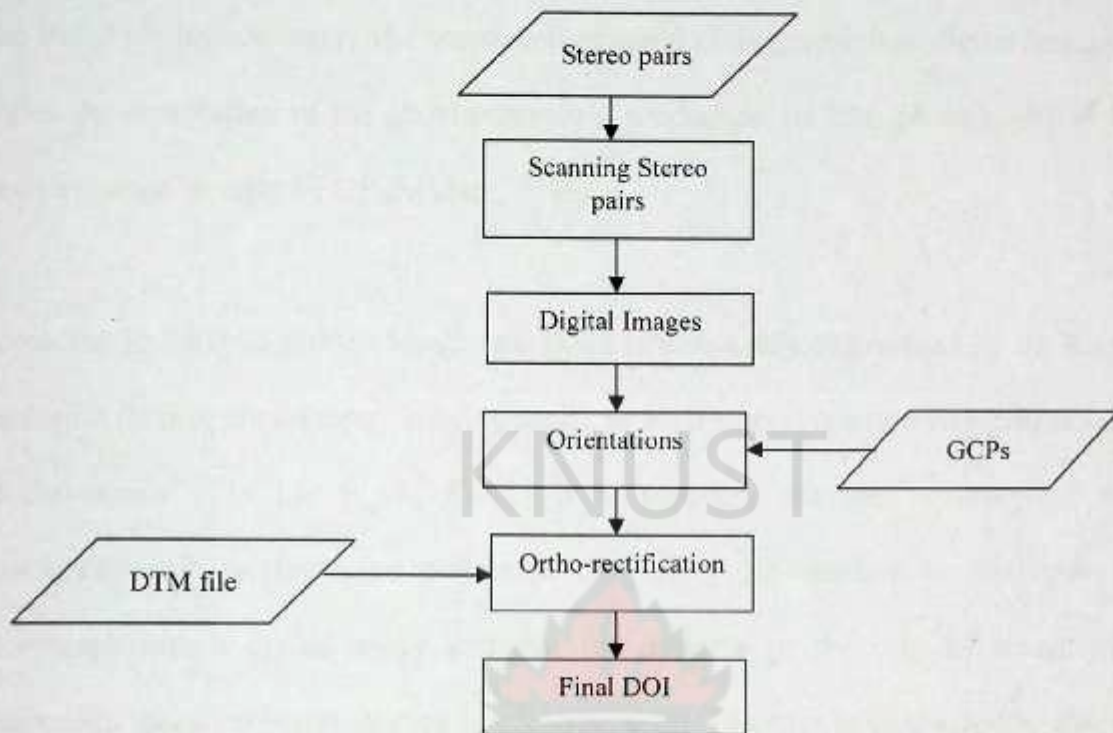
Figure 2-1: Schematic Diagram showing Work flow of DOI creation

Source: (Helina, 2002)

2.4.1 Digital Image Acquisition

As stated in section 2.4, the primary input for DOI production is the digital image. This image is obtained indirectly by scanning aerial photographs or directly by the use of sensors and digital cameras (ERDAS, 2003; Shahin, 1994; Potůčková, 2004). There have been innovative developments in sensors and digital cameras hence their increased use in photogrammetry for digital image acquisition. In recent times, satellite images such as spot data are being extensively used due to their geometric resolution and secured availability (Baltsavias and Stallmann, 1992). Even so, satellite imagery cannot completely replace aerial photos due to their high resolution (Brovelli, et al., 2006)

11

Fallow and Murray (1992) reported that digital systems do not suffer from limitations of film based photogrammetry. The translation of aerial photographs into digital images thus begins the automation of the photogrammetric production (if film photography is being used) a change brought by DP (Madani, 1996).

According to ERDAS (2003), image resolution is commonly determined by the scanning resolution (if film photography is being used), or by the pixel (picture element) resolution of the sensor. In Li, et al., (2002) it is reported that the accuracy of digital photogrammetric products are subject to the ability to translate an analogue aerial photograph into a digital image and that the preserve of the original image quality determines the scanning resolution that can be used. In order to optimize the attainable accuracy of a solution, the scanning resolution must be considered (ERDAS, 2003). The appropriate scanning resolution is determined by balancing the accuracy requirements versus the size of the mapping project and the time required to process the project (ERDAS, 2003). Resolution is either expressed as dots per inch (dpi), microns (μ) (adopted for this study) or in terms of ground distance.

Histograms can be developed for the scanned images and is used to adjust their radiometric contrast in the creation of a more pleasing general image tone. Due to large amount of image data, an image pyramid is usually adopted during the image matching techniques to reduce the computation time, increase matching reliability in order to decrease radiometric differences between image patches (ERDAS, 2003; Potůčková, 2004). The pyramid is a data structure consisting of the same image represented several times, at a decreasing spatial resolution (ERDAS, 2003).

12

2.4.2 GCPs

'One of the basic problems of photogrammetry is the reconstruction of the elements of the EO' (Steinbach, 1994). To solve this problem, GCPs are supplied to be used to determine the EO elements of each photograph (Li, et al., 2002). The minimum GCP requirements for an accurate mapping project vary with respect to the size of the project (ERDAS, 2003). I n establishing the mathematical relationship between image space and object space, seven parameters defining the relationship must be determined (ERDAS, 2003). The seven parameters include a scale factor (describing the scale difference between image space and ground space); X, Y, Z (ground coordinates defining the positional differences between image space and object space); and three rotation angles (omega (ω), phi (φ), and kappa (κ)) that define the rotational relationship between image space and ground space (ERDAS, 2003).

In order to compute a unique solution, at least seven known parameters must be available. When two X, Y, Z GCPs and one vertical (Z) GCP are used, the relationship can be defined. However, to increase the accuracy of a mapping project, using more GCPs is highly recommended (ERDAS, 2003).

The following descriptions are provided for various projects: If processing one image for the purpose of ortho-rectification (i.e., a single frame ortho-rectification), the minimum number of GCPs required is three. Each GCP must have an X, Y, (horizontal control) and Z (vertical control) coordinate associated with it. The GCPs should be evenly distributed to ensure that the camera/sensor is accurately modelled (Li, et al., 2002; ERDAS, 2003).

13

Some of the commonly used GCP features on the Earth's surface in photogrammetry include: intersection of roads, natural utility infrastructure (e.g., fire hydrants, corner of building and manhole covers), survey benchmarks and intersection of agricultural plots of land (ERDAS, 2003; Steinbach, 1994).

Depending on the type of mapping project, GCPs can be collected from a number of sources including: Planimetric and topographic maps (accuracy varies as a function of map scale), Theodolite and Total station survey (millimetre to centimetre accuracy) and global positioning system (GPS) survey (centimetre to meter accuracy) (ERDAS, 2003). GPS technology has allowed for a decrease in the time and cost of GCPs required for DOI production. In the last few years however, airborne GPS technology where GPS and an inertial navigation system (INS) or inertial measurement unit (IMU) are being used for direct Georeferencing to avoid GCPs and decrease time and cost (Steinbach, 1994; Wan, 2004 cited in Zhang and Yuan, 2008).

2.4.3 Camera Calibration Parameters

Another important input, the Camera Calibration Parameters, can be obtained from the Camera Calibration Certificate of the aerial camera used. Precision aerial cameras are periodically subjected to an inspection and a Camera Calibration Report is prepared. The report contains the coordinates of the fiducial marks given in a rectangular system. It also contains the focal length of the camera chosen so as to minimize the square sum of the measured distortion. The length from the principal point to the perspective center is called the focal length (Wang, 1990 cited in ERDAS, 2003).

Lens distortion deteriorates the positional accuracy of image points located on the image plane. Two types of lens distortion exist: radial and tangential lens distortions. The values of the distortion are referred to the calibrated focal length and to the principal point of symmetry. The effects of lens distortion are commonly determined in a laboratory during the camera calibration procedure (ERDAS, 2003) and are recorded in the camera calibration report. The principal point of autocollimation and the fiducial center all given in rectangular coordinate systems are stated in the calibration report supplied by the manufacturer for use during the DOI generation process.

2.4.4   Model Orientation

The photogrammetric exploitation of aerial images essentially requires the accurate reconstruction of the imaging geometry (Helina, 2002). For the camera positions in object space to be accurately reconstructed, the interior orientation (IO), the relative orientation (RO) and the absolute orientation (AO) are a prerequisite.

IO establishes a relationship between scanning coordinate system and image coordinate system rectifying existing errors in the digital image. This establishes a 2-D transformation that converts the scanned pixel coordinates to photo coordinates (Schenk, 1999 cited in Helina, 2002). The IO parameters are usually taken from a camera calibration report but can also be determined during the process of EO (by self-calibration) (Potůčková, 2004). The positions of fiducial marks, principal point location and lens distortion factors (See section 2.4.3) are input into the transformation equation. A reference marker is used to identify the fiducial marks on the screen of a workstation.

The software re-samples the radiometric matrix causing it to be in a new database related to the fiducial marks. Figure 2-2 shows the internal geometry of a camera. According to Li, et al., (2002) as with most DPS, accuracy report of IO is real time offered.

Figure 2-2: Schema of IO showing internal Geometry of camera
Source: (ERDAS, 2003).

In order to relate a model to the real terrain surface, the stereo pairs must go through EO. The elements of EO define the characteristics associated with an image at the time of exposure (ERDAS, 2003). This can be measured directly using INS or IMU (Steinbach, 1994). This orientation of stereo pairs can also be completed in two steps: RO and AO. The purpose of RO is to determine the relative positional relationship between two stereo pairs. RO includes three steps; conjugate points are searched for through image matching. This can be more precise than stereoscopic measurement in an analytical plotter if the aerial photograph has a good quality (Ackermann, 1994).

16

In the second step conjugate points are used to compute RO elements (x, y, z, ω, φ, and κ as shown in Figure 2-3) and finally, the three-dimension coordinates of the conjugate points are computed. The angular or rotational elements of EO describe the relationship between the ground space coordinate system (X, Y, and Z) and the image space coordinate system (x, y, and z).

The aim of AO is to relate image space to object space. This process can be completed through a transformation of coordinates using GCPs. It should be noted that the accuracy of orientation is determined mainly by accuracy of image matching and accuracy of GCPs (ERDAS, 2003; Li et al., 2002). Figure 2-3 shows the elements of EO.
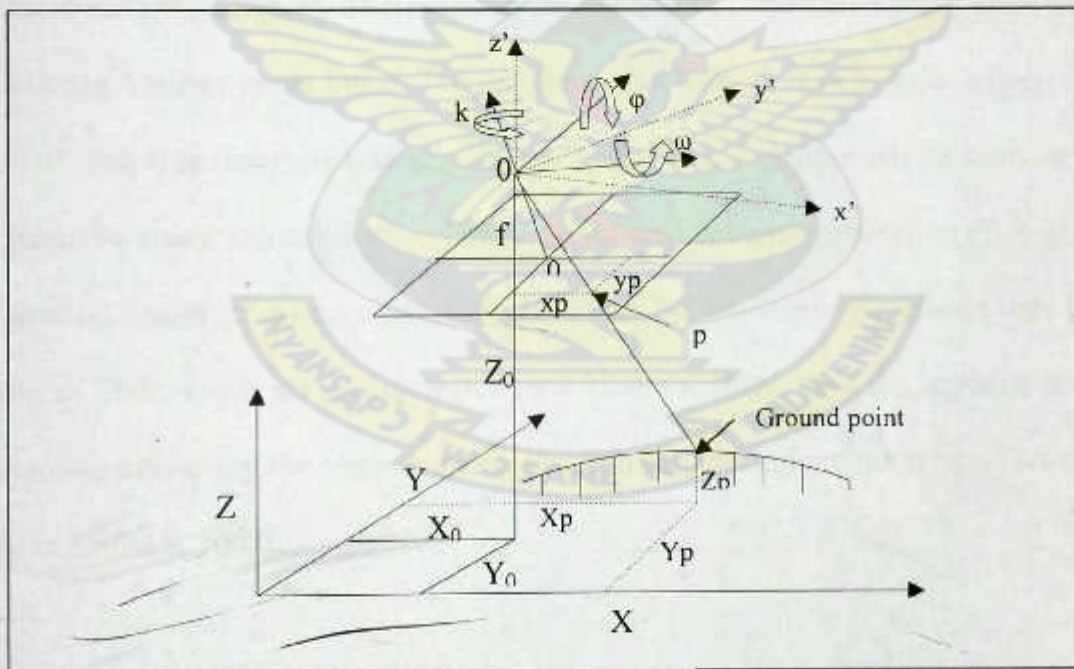
Figure 2-3: Schema of the elements of EO: RO and AO

Source: (ERDAS, 2003)

2.4.5 Generation of DEM

DEM is fundamental contents of any modern Geo-Information System (Buyuksalih et al., 2004). The United States Geological Survey (USGS) defines a DEM as a digital cartographic representation of the elevation of the terrain at regularly spaced intervals in x and y directions using z-values referenced to a common vertical datum (Maune et al. 2007 cited in McDougall, et al., 2008) The role of the DEM is to eliminate terrain induced displacement so as to transform a central perspective photograph to an orthogonal projection (Li, et al., 2002). There are two commonly available DEMs: grid based (used in this study) and triangulated irregular network (TIN) (McDougall, et al., 2008).

The quality of photogrammetrically generated DEMs depends on a number of factors which include the accuracy of elevations, the accuracy of image matching and spacing of the elevation points in the DEM. The required point density is in practice selected on the basis of sampling theory (Li, et al., 2002). Several re-sampling methods such as nearest neighbor, by-linear and cubic convolution can be used in image processing (Takagi, 1998). Theoretical and practical investigations show that the re-sampling methods based on the Gaussian filter, which are approximated by a binomial filter, have the superior properties concerning preserving the image contents and reducing the computation time (Wang, 1994 cited in ERDAS, 2003).

DEM can be obtained in several ways, including stereo matching from an aerial photograph or a satellite image (method used in this study), an interferometry from Synthetic Aperture Radar (SAR) and interpolation from a topographic map. Also USGS offers digital chart of the world that has elevation. Each DEM has various grid sizes and

18

various elevation accuracies (Takagi, 1998). The grid spacing is not dependent on an interpolation scheme where DEM is automatically produced by image matching (method used in this study). The accuracy of the automatically generated DEM is generally much better than that from conventional methods (Li, et al., 2002).

The final DOI is generated using the process of ortho-rectification which differentially transforms on a pixel-by-pixel basis, a central perspective image to an orthogonal image. This approach is a rigorous rectification in that it takes into account directly the ground surface elevation variation by incorporating into the solution the gridded DEM (e.g., Mayr and Heipke, 1988 cited in Chen and Lo, 2001).

2.5   Problems of DPS for the production of DOIs

Although most of the rigorous photogrammetric tasks in DP for DOI production have been computerized, there still exist lists of problems since it is in its early years. This study mainly precincts itself on the accuracy and use of DOIs which is the subject of the subsequent sub-sections.

2.5.1 Accuracy of DOIs

Although DPS can efficiently produce DOIs, its accuracy is doubted (Li, et al., 2002). This is because as stated in section 2.4, the production process of DOI involves many steps and requires multiple input data sets which add to the error of the final product. Throughout the DOI process, a wide range of these factors can affect the integrity of the final product.

19

The input data as discussed in sections 2.4.1, 2.4.2 and 2.4.3 forms the basis for DEM computation and automatic measurements such as image matching. The quality of the input data is thus of primary concern. Properties of digital images such as geometric quality, radiometric resolution, spatial resolution and spectral properties are affected by factors such as flight, camera Characteristics, imaging geometry, scale, photographic processing, scanner and pixel size (Honkavaara, et al., 1998; U.S. Department of the Interior, 1996) and hence should be done meticulously. In addition, the cost of scanners or its services push the initial cost of DP too high for higher accuracy and better interpretability since high scan resolution is mostly required (Walker, 1997).

The accuracy of orientation is of interest since it relates to the accuracy of relation between the ground and the image, which eventually affects the accuracy of the final DOI. Relative accuracy of orientation and thus DOI is related to photo scale (enlargement), image quality, camera calibration, mathematical model, and computation method but its absolute accuracy depends largely upon the quality of the GCP used (Honkavaara, et al., 1998). GPS is being widely used for measuring GCPs. GPS associated errors (multipath, ionospheric delay, errors of EO where direct georeferencing (INS or IMU) is used) (Li et al., 2002; Zhang and Yuan, 2008) should be eliminated as much as possible.

The effect of DEM on planimetric accuracy of DOIs cannot be overemphasized. Relative feature accuracy of DOI is based on the accuracy of the DEM. The relative accuracy cannot be more accurate than the accuracy of the DEM. The quality of DEM is affected by terrain type, quality of mapping method and interpolation method (see Section 2.4.5) used for ortho-rectification (Honkavaara, et al., 1998).

The enlargement from the aerial photo scale to the final DOI is crucial in the production process. The Map (e.g., DOI) scale depends on the scale of the aerial photography and the scale of the enlargements used for the planimetric mapping (PaMAGIC, 2002). The enlargement factor may vary between 4 to 10 times the photo scales.

2.5.2 Accuracy analysis of DOIs

Good science requires statements of accuracy by which the reliability of results can be understood and communicated (Zhang and Sun, 2002). For the products of DP to be widely accepted, it is necessary to analyze and prove their accuracy. Where accuracy is known objectively, then it can be expressed as error, where it is not, the term uncertainty applies (Hunter and Goodchild, 1993 cited in Zhang and Sun, 2002). Accuracy refers to the maximum error to be expected in the values of a dataset. It refers to the measure of correctness, which is comparing a sample of the data against reference information of known higher accuracy (Charlton and Frosh, 2008). The accuracy of a DOI can be analyzed with several methods; combinations of these methods are used in this study.

Positional Accuracy refers to the measurements of the location and size of features identified in an image. Positional accuracy has two main components: *Horizontal Accuracy* (the horizontal difference between a test point on an image and its true location) and *Vertical Accuracy* (the elevation difference between the test point and the true position). Vertical accuracies are used in reference to topographic imagery, such as contours (Charlton and Frosh, 2008). This research studies primarily horizontal accuracy.

21

The relative method of DOI accuracy assessment can be measured by comparing it to corresponding planimetric data (where ground features are visible). The DOI could also be edge matched against adjacent DOIs, and the relative displacement quantified. When a DOI is compared to adjacent DOIs, the relative accuracy specification of the adjacent DOIs should be based on the absolute accuracy specification (Scott, 2002).

Absolute DOI accuracy is quantified by measuring the distance between the position of ground features in the DOI and their true position on the ground. The number of GCPs required for this process will vary, depending on the accuracy standard. The desire is however to show a good statistical indication of overall accuracy (Scott, 2002).

Threshold accuracy refers to the minimally acceptable data accuracy values for products, applications, and contracting services supplied to or developed by governments. Threshold accuracy is generally stated as a numeric value that is the starting point of acceptable accuracy (Charlton and Frosh, 2008).

Classification Accuracy is the accuracy with which a feature is identified as belonging to a specific type or class such as forest or water. Classification accuracy is also referred to as attribute or thematic accuracy (Charlton and Frosh, 2008).

Ground Sample Distance (GSD) is defined as the distance across the area on the ground represented by a side of one pixel. An image that has a small GSD value exposes more detail, and is said to have a higher resolution. GSD does not always necessarily affect accuracy though it affects interpretability (Charlton and Frosh, 2008).

22

Root Mean Square Error (RMSE) is the square root of the average of the set of squared differences between dataset coordinate values and coordinate values from an independent source of higher accuracy for identical points (Scott, 2002; Charlton and Frosh, 2008). In this study, RMSE is used as a measure of planimetric (horizontal) accuracy and were computed using equations 2.1, 2.2 and 2.3.

$$\sigma(planimetry) = Sqrt(\sigma_x^2 + \sigma_y^2) \qquad\qquad 2.1$$

$$\sigma_x = \sqrt{\frac{\sum(\Delta x)^2}{n}} \qquad\qquad 2.2$$

$$\sigma_y = \sqrt{\frac{\sum(\Delta y)^2}{n}} \qquad\qquad 2.3$$

Where: σ = Planimetric RMSE, σ_x= RMSE in X (RMSEx)

σ_y= RMSE in Y (RMSEy)

Δ_x= difference between X coordinates of Checkpoints and Measured Points from DOI

Δ_y= difference between Y coordinates of Checkpoints and Measured Points from DOI

The National Standard for Spatial Data Accuracy (NSSDA) was developed to estimate positional accuracy.The NSSDA's absolute accuracy statistics is computed from RMSEs using equation 2.4 in order to report tested horizontal accuracy at 95% confidence level where $\sigma_y \neq \sigma_x$ and RMSEmax/RMSEmin is between 0.6 and 1.0 (Federal Geographic Data Committee (FGDC), 1998).

Accuracy $\approx 2.4477 \times 0.5 \times (\sigma_y + \sigma_x)$ $\qquad\qquad 2.4$

The United States National Map Accuracy Standards (NMAS) on horizontal accuracy states that, for a map to meet accuracy standards 90 percent of the well-defined points tested must fall within (1/50 inch) of a small scale map (<1:20,000) and (1/30 inch) of a large scale map (>1:20,000) (FGDC, 1998). Following in Table 2-1 are the scales for mapping as per NSSDA and NMAS

Table 2-1: Accepted spatial accuracy values as per NSSDA and NMAS

Map Scale (ft and m)	NMAS CMAS 90% confidence level Maximum Error Tolerance (ft)	NSSDA RMSE (ft and m)	NSSDA Accuracy at 95 % confidence level (ft and m)
1" = 100' or 1:1,200	3.33	2.20 or 0.671	3.80 or 1.159
1"=200 or1:2,400	6.67	4.39 or 1.339	7.60 or 2.318
1" = 400 or 1:4800	13.33	8.79 or 2.678	15.21 or 4.635
1" = 500 or 1:6000	16.67	10.98 or 3.348	19.01 or 5.794
1" = 1000 or 1:12000	33.33	21.97 or 6.695	38.02 or 11.588
1" = 2000 or 1:24000	40.0	26.36 or 8.035	45.62 or 13.906

Source: (Charlton and Frosh, 2008)

2.5.3 Analysis of use of DOI based on Accuracy

The use of DOIs can be determined if their accuracy to a greater extend is known. Their use can then be depicted by relating their accuracies with horizontal accuracy of maps. The horizontal accuracy of a map is related to the map scale which determines how well features on the map correspond to their 'real world' counterparts. For DOIs to be used for solving 'real world' problems they must be related to and must meet accuracy standards of large and or small scale maps for which they are to be used (PaMAGIC, 2002).

24

CHAPTER THREE

MATERIALS AND METHODS

3.1 Introduction

This section proceeds to describe the resources (including the data acquired) used in this study, the data acquisition methods employed, the types of DOIs generated and concludes with the accuracy analysis methods of the DOIs used.

3.2 Resources

A Vexcel Ultra Scan 5000, Photogrammetric Scanner, was used to scan the diapositives used in this study. The DOI production process was performed on a Dell Digital Photogrammetric Workstation (DPW) of a hard disc size of 10TB (with RAID5), a RAM of 2GB and a speed capacity of 1GB linked to a DELL Precision 690, 2x5 TB server, 139H/USB, CHA 1200FU/800FU. A desktop computer of hard disc size 73GB, a RAM of 0.99GB and speed of 2.99Hz was used for the measurements for accuracy analysis. A SOKKIA Radian IS geodetic-grade GPS was used for the observation of GCPs for this study.

An INPHO photogrammetric software 'Application master' version 5.0.2 was used for the generation of the final DOI types. The Geometric orientations of the final DOI for the relative accuracy analysis and analysis of use of DOI as well as all measurements for absolute accuracy analysis were done with ArcGIS 9.1. Spectrum® Survey 3.50 was used for processing the GPS data collected for this study. Microsoft Excel software was used for the statistical analysis and for plotting statistical charts. During the study, Windows XP was the main operating system used.

25

3.3 Data Acquisition and Processing

Two digital stereo pairs of aerial photographs and 25 GCPs from GPS survey were used in this study. The aerial photographs for this study were obtained from a set of aerial photographs, taken by FINMAP, FM-INTERNATIONAL. For the purpose of this research, two aerial photos of numbers 2561 and 2562 of roll 6, run 15A were used. The detail specification of the 20 microns TIFF files stereo pairs are shown in Table 3-1. The camera calibration certificate as well as the aerial photography film report can be obtained in appendix 2 and 3a-3e respectively.

Table 3-1: Flight and block data of input images used in research

Study Area	Portions of Kentinkrono-Nsenia
Area covered	About 2.00km x 1.00m
Ground height	265-275m
Flying height above sea level	Approx. 1,830m
Camera used	Leica RC 30
Photo scale	1:10000
Forward/side overlap	60%/25%
Number of strips	1
Number of images	2
Date of flight	1st May, 2008
Time of flight	9:40am-11:50am
Film type	Kodak colour III 2444
Image scan resolution	20 microns
Principal distance/digital image type	152.86mm/RGB
Terrain Characteristics	Urban, Hilly with valleys and plains

The GCPs for the orientation and accuracy analysis in this study were acquired with a Geodetic-grade GPS. The method of Differential Global Positioning System (DGPS) was used for the observation and processing of GCPs. A pre-marked flagged (Figure 3-1.) Photogrammetric Ghana Reference Network (GRN) control point (SGA13/07/12) of known coordinates was used as a base station for processing the GCPs (see appendix 7 and 6b for GCPs used and their corresponding root mean square (RMS) respectively).

Figure 3-1: A Flagged Photogrammetric Control Point

Mainly road intersections and junctions (e.g., see appendix 4) located in the overlap area of the stereo pairs which could be found on the field were identified and observed for use as GCPs. Each GCP station was occupied for not less than 20 minutes (see field bookings in appendix 5) with the GPS during their observation. The WGS 84 ellipsoid was adopted for this study.

3.4 How DOIs were Generated

The digital images acquired (mentioned in Section 3.3) were loaded into the photogrammetric software and map units as well as map projections were specified. The needed information (as mentioned in Section 2.4.3) from the camera calibration certificate was inputted. The GCPs (see Appendix 7) were supplied followed by the approximate projection centres. A standard deviation setting was defined and a consistency check of all project definitions was performed. Image pyramids (see Section 2.4.1) were created for the loaded images and their colour/brightness and contrast were enhanced using the 'image commander' of the photogrammetric software. An automatic AT was done using MATCH-AT (part of INPHO software for this process) (Kaczynski and Ziobro, 1998).

27

IO was done in the software automatically by measuring the fiducial coordinates of the camera. Details of results of IO and a summary of AT statistics can be obtained in appendix 8 and 9 respectively.

Using processes as mentioned in Section 2.4.5, the DEM was generated using MATCH-T (part of INPHO software for this process) with optimum parameters and used for the orientation of the stereo pairs to create the final DOI. A constant DEM grid interval was used for all DOIs generated except for the DOI generated for purposes of the study of the effect of different grid intervals on DOI accuracy.

3.4.1 Types of DOIs generated

In all 10 DOIs were created based on the different conditions set and were used for the various analysis.

Three DOIs were generated from three Different numbers of GCPs. During this process a constant DEM grid interval of 6m and a constant scale of 1:10,000 were ensured. The number of GCPs used for the different DOIs created included; 10, 7 and 4 GCPs respectively.

In addition, the DEM grid interval was then varied for the creation of three other DOIs at a constant scale of 1:10,000 using 10 GCPs. DEM grid Intervals 9m, 12m and 50m were selected for use.

Also three Different scales were used to create three DOIs using 10 GCPS and a constant DEM interval of 6m. For the variation in scale, photo scales; 1: 2,500, 1: 5,000 and 1:10,000 corresponding to ground pixel sizes of 0.05m, 0.1m and 0.2m respectively were selected for use.

Finally a DOI for relative accuracy and analysis of use was generated using the 10 GCPs, a DEM grid interval of 6m and a scale of 1:10,000. The DEM for the creation of this DOI was edited with the use of breaklines (See appendix 13) to ensure that majority of the mass points were corrected.

3.5   Analysis of Accuracy and Use of DOIs Produced

The methods stated in Sections 2.5.2 and 2.5.3 were used for the analysis of accuracy and use of DOIs. RMSE values obtained in this study were compared with standard values (see Table 2-1) and used for the analysis extensively dealt with in the next chapter.

CHAPTER FOUR

RESULTS AND ANALYSIS

4.1 Introduction

This Section looks at the results acquired in this study and the methods used for their analysis leading to the conclusions and recommendations drawn. The analysis included all the results obtained in the various processes (such as GCP processing) and the final results obtained from the computed RMSEs of the different types of DOIs created.

4.2 Results

Apart from the results reported in this section, reference is made to results in other sections of this thesis as and when necessary. Using equations 2.1, 2.2, 2.3 and 2.4 in Section 2.5.2, the RMSE and accuracy of the DOIs were computed as per NSSDA 95% confidence level and the result is shown in Table 4-1. The detail computation including the discrepancies of GCPs for the different DOIs created can be found in Appendix 11. The accuracy results obtained for the DEM extraction are found in Table 4-2.

Table 4-1: Computed RMSE and Accuracy as per NSSDA

DOI Type	Sum of square discrepancies		Mean Square Error		RMSExy (σxy) (m)		RMSE (m)	Accuracy (m)
10 GCPs	11.443	9.299	0.817	0.664	0.904	0.815	1.217	2.104
7GCPs	23.701	9.327	1.693	0.666	1.301	0.816	1.536	2.591
4GCPs	13.987	28.601	0.999	2.043	1.000	1.429	1.744	2.973
9m DEM	13.251	8.500	0.947	0.607	0.973	0.779	1.246	2.144
12m DEM	13.437	9.338	0.960	0.667	0.980	0.817	1.275	2.199
50m DEM	12.015	10.921	0.858	0.780	0.926	0.883	1.280	2.214
2500sc	13.493	9.173	0.964	0.655	0.982	0.809	1.272	2.192
5000sc	13.346	10.039	0.953	0.717	0.976	0.847	1.292	2.232
10000sc	12.955	11.068	0.925	0.791	0.962	0.889	1.310	2.265
Edited DEM	7.350	9.299	0.525	0.664	0.725	0.815	1.091	1.884

Table 4-2: Accuracy results of the DEM extraction

DOI Type	Internal height accuracy(m)	Time elapsed(s)
10 GCP DOI	0.081331	4
7 GCP DOI	0.081523	4
4 GCP DOI	0.081894	4
9m DEM grid int.	0.081331	4
12m DEM grid int.	0.081331	3
50m DEMgrid int.	0.081331	1
10000 scale	0.081331	4
5000 scale	0.081331	4
2500 scale	0.081331	4
Edited DEM	0.081331	4

4.3 General comments and Analysis of Results

The results were analyzed and evaluated with the criteria of accuracy and use of DOI based on accuracies obtained. The RMSs obtained from the IO operation (see Appendix 8) and those from the processing of GCPs (see Appendix 6b) were generally acceptable for use. From Table 4-1 it could be seen that the planimetric accuracies (RMSE) of all the DOIs produced were less than 1.500 pixels except the DOIs produced from 7 GCPs and 4GCPs which were 1.536 and 1.744 respectively. Generally majority of values were acceptable within the stated standards (see Section 2.5.2).

The DEM accuracy results in Table 4-2 revealed that errors obtained was constant for all the DOIs generated except DOIs generated with different number of GCPs. The error was at highest for the DOI generated with the least number of GCPs (4GCPs DOI). In addition, the time used was constant for all except that it reduced when the DEM grid interval was increased.

31

Also from Appendix 9, results showed that, when a greater number of GCPs were used, the standard error in ω, φ, and κ values minimised. Reduction in the number of GCPs resulted in an increase in the standard deviation and hence sigma naught values.

4.3.1 Analysis of DOI Accuracies Obtained

The accuracy analysis proceeded in two main ways; the DOI was compared with an existing line map and the RMSEs of the different DOIs were computed for further analysis. In the relative analysis, the DOI created with edited DEM was used. The DOI was geometrically corrected (See Appendix 10 for RMSE values) and a line map of the same area was superimposed on it. Most of the features of the line map fell on their corresponding features in the DOI (Figure 4-1).

Figure 4-1: DOI showing superimposed line map

A careful look at the result however showed that even though most of the features were in their exact positions in the DOI, few features were in error of about 1.000m to their corresponding features on the ground (Figures 4-2). Some features on the line map could not be found on the DOI due to reconstruction since it was created with aerial photos of higher currency than the line map (Figures 4-3).

Figure 4-2: DOI showing better line map superimposition

Figure 4-3: A portion of DOI showing reconstruction

In order to properly quantify the errors in the DOIs, from RMSE obtained, accuracy of each DOI was computed (shown in Table 4-1) and compared with accuracy standard values as per NSSDA (shown in Table 2-1). For the accuracy of the DOIs created to be acceptable, their accuracy values should be within the range of standard values specified in Table 2-1. The bigger these values the poorer the accuracy of the DOI. Considering the conditions at which the DOIs were generated (see Section 3.4.1), their accuracy values were acceptable for use for the subsequent analysis.

For further analysis of variation in accuracy, the DOI created with edited DEM was selected as the basis for comparison with other DOIs since it had a better RMSE and accuracy values (see Table 4-1). Comparing the accuracy of DOI created with edited DEM and the DOIs created with the selected parameters resulted in Table 4-3.

Table 4-3: Accuracy difference between each DOI and DOI from edited DEM

DOI created with	Difference in RMSE as compared with edited DEM DOI(m)	Difference in Accuracy as compared with edited DEM DOI(m)
10 GCPs	0.126	0.220
7GCPs	0.445	0.707
4GCPs	0.654	1.088
9m DEM interval	0.155	0.260
12m DEM interval	0.184	0.315
50m DEM interval	0.189	0.330
2500 software scale	0.181	0.308
5000 software scale	0.201	0.347
10000 software scale	0.219	0.381

From Table 4-3, it is evident that the differences were significant with the varying GCPs than those for varying DEM grid interval and varying scale.

34

The accuracy differences for DOIs created with 7 and 4 GCPs were 0.707m and 1.088m and RMSE differences were 0.445m and 0.654m respectively (see Table 4-3). The remaining DOIs had RMSE and accuracy differences less than 0.400m. This revealed that, the accuracy variation for the different DOIs created with different number of GCPs was relatively significant compared with the accuracy variation of DOIs from varied scale and varied DEM grid interval. Charts of the accuracy and RMSE of the various DOIs were plotted and used for further analysis.
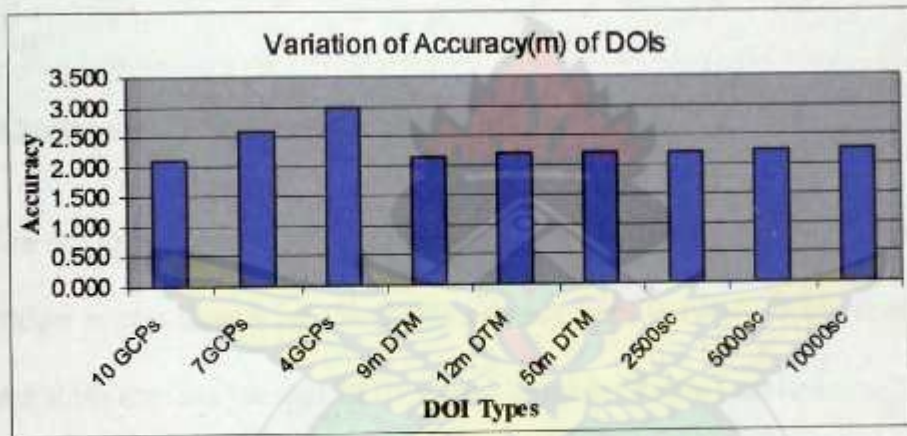
Figure 4-4: Chart showing accuracy differences of DOIs

Figure 4-4 describes the accuracy differences of DOIs. From this figure, it was seen that the DOI created with 4GCPs had the longest bar closing 3.000m depicting that it had the largest accuracy value. This was followed by the DOI created with 7GCPs and the rest of the bars were a little above 2.000m. This could imply that, there was a wide deviation of the DOIs created with 4 and 7GCPs respectively from the more probable value. The deviation was very significant with the DOIs created with fewer GCPs which had greater accuracy values than the others which had relatively more GCPs. The deviations of the DOIs created with the varying number of GCPs and DEM grid intervals, however, were

35

relatively insignificant as is depicted in Figure 4-4. Further analysis was made from plotted charts of the RMSE obtained.
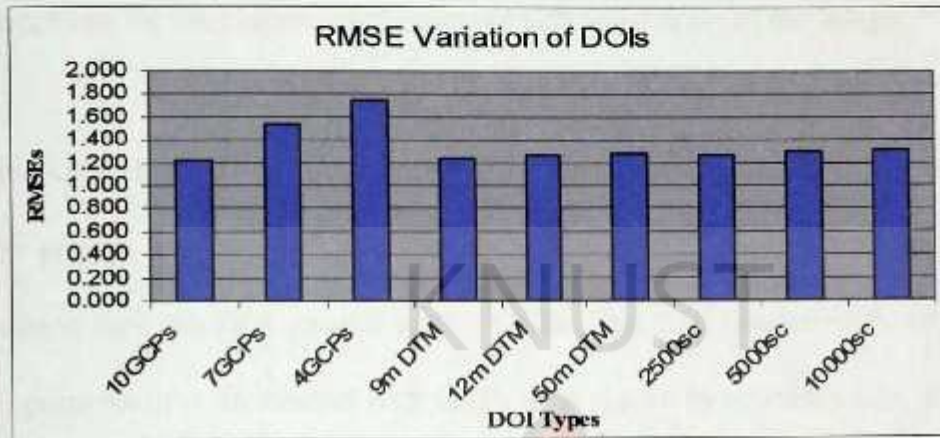
Figure 4-5: Chart showing RMSE variation of DOIs

From Figure 4-5 of varying RMSEs, it is seen that the RMSE deviation from the more probable value is significant for the DOIs created with varying GCPs than the others. Charts of the RMSE of the various DOIs were plotted for further analysis.
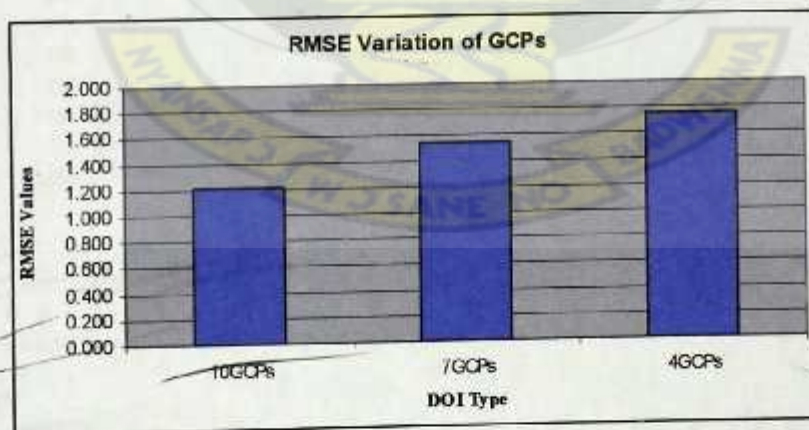
Figure 4-6: Chart showing variation of RMSE of DOIs created with varying GCPs

From Figure 4-6, again it could be seen that apart from the RMSE of 10GCP DOI being a little above 1.200m, the variations in the bars were significant with 4 and 7 GCP DOIs

going beyond RMSE of 1.500m. Together with the initial results from this study, it was clear that a change in the number of GCPs had a significant effect on the accuracy of DOI produced. This could imply that the additional GCPs used for the creation of the 10 GCP DOI gave options for the placement of points in almost all areas of the image.

Also from Appendix 12(a-c), considering that even distribution of GCPs used in the orientation process was ensured, the DOI created with 7 GCPs had more points in the central portion than the DOI created with 4 GCPs. The DOI created with 10 GCPs had almost all portions of it distributed with GCPs as is shown in appendix 12c. This implies that the location of GCPs in terms of their distribution is important in determining accuracy of DOIs (Zhang, 2002). This explains the reason for the significant variation of RMSE for DOIs created with varying GCPs.
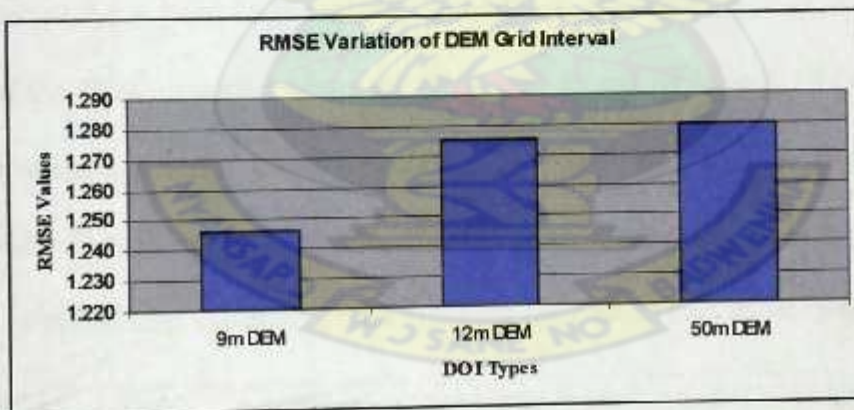
Figure 4-7: Chart showing RMSE of DOIs of varied DEM grid intervals

From the chart showing varying DEM grid interval (Figure 4-7) it can be seen that, the variation of RMSE for all the DOIs were within 1.240m and 1.280m. This insignificant

37

variation can be explained to mean that a variation in the DEM grid interval for DOI

creation has very little effect on the accuracy of the final DOI.
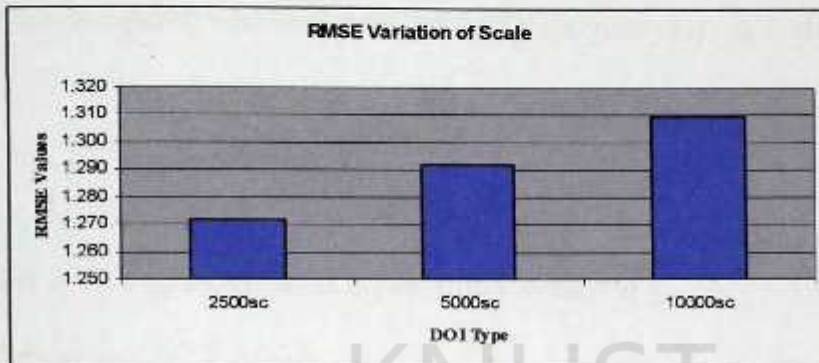
Figure 4-8: **Chart showing variation of RMSE of DOIs created with varying scale**

Figure 4-8 also showed an insignificant variation of RMSE from a little above 1.270m to

1.310m implying little effect on the accuracy of the final DOI generated. Comparing

Figure 4-7 and Figure 4-8, it could be seen that the variation of RMSE of DOIs created

with varying scale was relatively significant and thus would have relatively greater effect

on the accuracy of the final DOI created. In addition, the resolution as well as time of

production of the DOI increased when the scale was increased from 1:10,000 to 1:2,500.

The same amount of zoom caused pixilation in the 1:10,000 DOI making features

indistinct, while features of the 1:2,500 DOI could still be seen. A comparison of the

significance of the RMSE variation of the different conditions was made (see Figure 4-9).
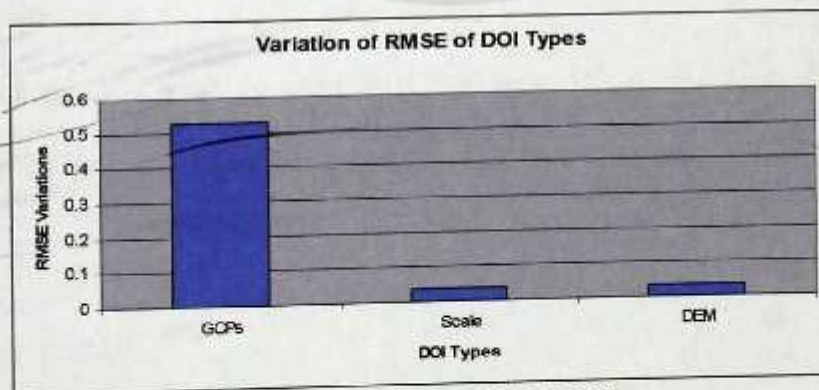
Figure 4-9: Chart showing significance of deviation of RMSE of DOIs

Finally the chart (Figure 4-9) which compares the differences in the largest and lowest RMSE of the various DOIs showed that the difference in RMSE from varied GCPs was very significant compared with the RMSE of the DOIs from varying scale and DEM grid interval.

4.3.2 Analysis of Use of DOIs based on accuracy obtained

The use of DOI based on accuracy was analyzed in two ways: The RMSE 1.091m obtained for the DOI created with edited DEM was used for this analysis. It was compared with the acceptable RMSE of NMAS values for small and large scale maps. For a map to meet accuracy standards of NMAS, 90 percent of the well-defined points tested must fall within (1/50 inches) for maps of scale $\leq$ 1:20,000 and (1/30 inches) for map scale $\geq$ 1:20,000. Using a small scale of 1:20,000 gave 33.3ft (10.160m). Compared with the RMSE of 1.091m of the DOI used qualified it for use as that small scale map.

Selecting a large scale map of scale 1:2500, the accuracy standard for large scale maps, (1/30 inch) gave $\leq$ 6.944feet (2.117m). Comparing this with the RMSE (1.091 m) of the DOI showed that it could be acceptable for use as the above large scale map. The scale when further increased to 1:1500, gave accuracy of $\leq$ 4.167ft (1.270m). Thus again suggesting that the DOI could be used as 1:1500 map. Finally the scale was increased to 1:500, and the accuracy resulted as $\leq$ 1.389ft (0.423m). The RMSE of the DOI failed at this scale.

In addition, measured distances of some features on the DOI at a fixed scale of 1:2500 were compared with their corresponding measured distances on vector map of the same scale. The results are shown in the Table 4-4.

Table 4-4: Differences between measured distances of DOI and Vector map

Feature name	Ground Distance(m)	DOI Distance(m)	Absolute Difference(m)
Fencing	11.7000	11.702	0.002
School block length	39.000	39.026	0.026
School block width	14.300	14.552	0.252
Length of culvert	18.020	18.110	0.090
Security post	3.800	3.590	0.210

From the Table 4-4, it was seen that at the scale of 1:2500, the measured distances on DOI compared to their map distances were significantly close. Together with earlier results in this Section, it is clear that the DOI could be used as a large scale map. Thus the uses of a large scale map could also apply to that of the DOI obtained.

40

CHAPTER FIVE

CONCLUSIONS AND RECOMMENDATIONS

5.1 Introduction

Photogrammetry has evolved to the digital phase due to the development and advancement in computer, camera, storage technologies and increased research. DP is being used in almost all areas of mapping; more especially its use for the production of DOIs has increased globally. The production of DOIs has increased as a consequence of the numerous advantages they have over other products. The accuracy of DOIs is thus critical to the producer as well as the user and has necessitated a global investigation.

An attempt was made in this research to find out the effect of some steps in DOI production on their accuracy and how the accuracy obtained could decide their use. This chapter presents the conclusions and recommendations made based on findings obtained.

5.2 Conclusions

Bringing together the main findings of the results obtained and analysis carried out, the objectives of the research were realized and the following conclusions drawn:

The DOI production process requires the supply of GCPs for orientating the digital image from image space to object space. It is important to understand the effect of this input on the accuracy of the DOI generated. Results of this research revealed that the difference in the RMSE obtained for the DOIs created with varying number of GCPs was very significant. This implies that when all conditions including: accuracy and even distribution

41

of GCPs are satisfied, the number of GCPs used for DOI creation should be critically considered. This is because the number of GCPs supplied for the orientation of the digital image significantly affects the accuracy of the final DOI obtained. The greater the number of GCPs used, the better the accuracy of the DOI. It is thus important to note that having a greater number of GCPs within all parts of the image has similar importance as the accuracy of the GCPs used and is a prerequisite to attaining better accuracies of the final DOI.

DEM is a fundamental content of any modern Geo-Information System which eliminates terrain induced displacement so as to transform a central perspective photograph to an orthogonal projection. Even though the accuracy of the DEM file among others used for the ortho-rectification of the digital image decides the accuracy of the DOI generated, the findings of this research show that the difference in the RMSE for DOIs created with varying DEM grid interval was not very significant. This implies that the choice of DEM grid interval has little significant effect on the accuracy of final DOI created.

The findings of this research also revealed that the difference in the RMSE for varying scale has little significance. It thus implies that unlike the number of GCPs used, the effect of the choice of scale has little significance on the accuracy of final DOI obtained. In addition, it was further revealed that the choice of scale is relatively critical (since this affected accuracy quite significantly) compared with the choice of DEM grid interval. This is because it was found that the variation in scale had a relatively high significant change on the RMSE obtained compared with the variation in the DEM grid intervals.

Also, even though the effect of the choice of scale on the accuracy of the final DOI is relatively insignificant (compared with number of GCPs); its effect on the quality (resolution) of the final DOI is significant. The larger the scale chosen in relation to the source scale, the better the resolution and the converse is true. However, the result of increasing the scale is that it increases production time of the DOI.

The right use of a DOI can be achieved if its accuracy relating to horizontal accuracy of maps to a greater extent is known. The horizontal accuracy of a map is related to the map scale which determines how well features on the map correspond to their 'real world' counterparts. Considering the result obtained for the use DOIs in this study, it is apparently evident that the accuracy of the DOI used was comparable to some small and large scale maps. This implies that, DOIs can be used for the purposes of small scale and some large scale maps. However, they cannot be used at scales beyond the allowable magnification of the source scale. It is gain saying thus that the use of DOIs should be within allowable scale enlargements since they cannot be used beyond certain magnification of the source scale from which they were produced.

5.3 Recommendations

The objectives of the research were attained. However, future research should investigate the following:

- The effects of interpolation algorithm on the accuracy of DOIs
- The effects of GCP location characteristics (nature of terrain) on the accuracy of DOIs

43

LIST OF REFERENCES

Ackermann, F., 1994. Digital elevation models--techniques and application, quality standards, development. In: Symposium on Mapping and Geographic Information Systems. *ISPRS*, Athens, Ga., Vol. 30(4), pp. 421-432.

American Society of Photogrammetry (ASP), 1980. *Manual of Photogrammetry.* 4th ed. Virginia Avenue: American Society of Photogrammetry.

Aspinall, R., Miller, D., Finch P., and Fon T. C., 1994. A Model of DEM and orthophotograph Quality Using Aerial Photography. *GIS/LIS '94 Proceedings*, Bethesda: ACSM-ASPRS-AAG-URISA-AM/FM, pp. 24-33.

Ayhan, E., Erden, Ö., Atay G., and Tunç, E., 2006. Digital Orthophoto Generation with Aerial Photos and Satellite Images and Analyzing of Factors which Affect Accuracy. *Shaping the Change*, XXIII FIG Congress Munich, Germany, Oct.8-13, pp. 1-14.

Baltsavias, E. P., 1995. Digital ortho-images - a powerful tool for the extraction of spatial- and geo-information. *ISPRS, Journal of Photogrammetry and Remote Sensing*, Vol. 51, Issue 2, April 1996, pp. 63-77.

Baltsavias, E. P., and Stallmann, D., 1992. Metric Information Extraction from Spot Images and the Role of Polynomial Mapping Functions. *Proceedings Of 17th ISPRS congress*, In: IAPRS, Washinton D. C., USA. Vol. 29, Part B4, Aug.2-14, pp. 358-364.

Brovelli, M. A., Crespi, M., Fratarcangeli, F., Giannone, F., and Realini, E., 2006. Accuracy assessment of High Resolution Satellite Imagery by Leave-one-out method. In: M. Caetano and M. Painho, ed. *Proceedings of the 7th International Symposium on Spatial Accuracy Assessment in Natural Resources and Environmental Sciences.* Lisbon, Portugal, Jul. 5-7, 2006, pp. 553-556.

Buyuksalih, G., Oruc, M., Topan, H., and Jacobsen, K., 2004. Geometric Accuracy Evaluation, DEM Generation and Validation for SPOT-5 Level 1B Stereo Scene. *EARSeL Workshop,, Remote Sensing for Developing Countries "Cairo*, 6 p.

Çakir, G., Keles, S., Sivrikaya, F., Başkent E, Z., and Köse, S., 2006. Determining the effects of different scanner and scanning resolutions on orientation errors in producing of Orthophotos. In: M. Caetano and M. Painho, ed. *Proceedings of the 7th International Symposium on Spatial Accuracy Assessment in Natural Resources and Environmental Sciences.* Lisbon, Portugal, Jul. 5-7, 2006, pp. 553-556.

Charlton, T., and Frosh, R., 2008. *Map Accuracy Definitions,* United States Department of Agriculture, [online]. Available at: < URL: http://www.itc.nrcs.usda.gov/scdm/docs/SPG-MapAccuracyDefinition.pdf> [Accessed February, 2009].

Chen, L.-C., and Lo, C.-Y., 2001. Generation of Digital Orhtophotos from Ikonos Geo Images. *Paper presented at the 22nd Asian Conference on Remote Sensing, Nov. 5-9,* Centre for Remote Imaging, Sensing and Proceeding (CRISP), National University of Singapore, 6p.

Cory, M. J., and Mcgill, A., 1999. DEM Derivation at Ordinance Survey Ireland. *OEEPE*, Official publication No. 37, pp.189-208.

ERDAS, 2003. *ERDAS Field Guide*. 7th ed. Leica Geosystems GIS and Mapping LLC, Atlanta, GA, pp. 265-303.

Fallow, J. E., and Murray, K., 1992. Digital Photogrammetry: Options and Opportunities. *International Archives of Photogrammetry and Remote Sensing*, Vol. 29, Part B2, pp. 397-403.

Federal Geographic Data Committee (FGDC), 1998. Geosp atial Positioning Accuracy Standards. *National Standard for Spatial Data Accuracy*, Part 3, FGDC-STD-007.3-1998, pp. 1-25.

Fletcher, C., Rooney, J., Barbee, M., Lim, S. C., and Richmond, B., 2003. "Mapping shoreline change using digital orthophotogrammetry on Maui, Hawaii", *Journal of Coastal Research, Special Issue,* Vol. 38, pp. 106-124.

GEOSYSTEMS, 2004. *Scientific Production Enterprise.* Digitals Photogrammetric Station (Delta), [online]. Available at: < URL: www.vingeo.com/images/DPS.jpg> [Accessed 24 February 2008].

Helina, O. A., 2002. *Optimising the workflow in a Hybrid Production System of Analytical and Digital Production of Geodata from Aerial Photographs.* Master thesis, International Institute for Geo-Information Science and Earth Observation ENSCHEDE, The Netherlands, 66 p.

Honkavaara, E., Kaartinen, H., Kuittinen, R., Huttunen, A., and Jaakkola, J., 1998. The Quality control in the finish land parcel identification system orthophoto production (FLPIS). In: D. Fritsch, M. Englich, and M. Sester, ed. *ISPRS commission IV symposium on GIS-Between versions and applications,* IAPRS' Stuttgart, Germany, Vol. 32/4, 8 p.

Kaczynski, R., and Ziobro, J., 1998. Digital Aerial Triangulation for DTM and Orhtophoto Generation. In: D. Fritsch, M. Englich, and M. Sester, ed. *ISPRS commission IV symposium on GIS-Between versions and applications,* IAPRS' Stuttgart, Germany, Vol. 32/4, pp. 281-283.

Konecny, G., 1985. "The International Society for Photogrammetry and Remote Sensing – 75 Years Old, or 75 Years Young". *Keynote Address, Photogrammetric Engineering and Remote Sensing,* Vol. 51(7), pp. 919-933.

Li, D., Gong, J., Guan, Y., and Zhang, C., 2002. Accuracy Analysis of Digital Orthophotos, *ISPRS, Commission II, Symposium 2002*, Vol. XXXIV, Part 2, XI'an, P. R. China, Aug.20-23, pp. 241-244.

Madani, M., 1996. Digital Aerial Triangulation – The Operational Performance. *Presented at the XVIII ISPRS congress*, Vienna, Austria, July 9-19, 1996. Moore, L. J., 2000. "Shoreline mapping techniques". *Journal of Coastal Research*, Vol. 16, pp. 111-124.

McDougall, K., Liu, X., Basnet B., and Apan, A., 2008. Evaluation of Current DEM Accuracy for Condamine Catchment. In: Wan, Y. et al., ed. *Proceedings of the 8th International Symposium on Spatial Accuracy Assessment in Natural Resources and Environmental Sciences*. Shanghai, P. R. China, June 25-27, 2008, World Academic Union (Press), pp. 71-78.

Potůčková, M., 2004. *Image Matching and Its Applications in Photogrammetry*. PhD. Thesis, Aalborg University, Fibigerstraede 11, DK-9220 Aalborg, Denmark, pp.1-5.

Sarjakoski, T., 1981. Concept of a Completely Digital Stereo Plotter. *The photogrammetric journal of Finland*, Vol. 8, No. 2, pp. 95-100.

Schickler, W., and Thorpe, A., 1998. Operational Procedure for Automatic True Orthophoto Generation. In: D. Fritsch, M. Englich, and M. Sester, ed. *ISPRS commission IV symposium on GIS-Between versions and applications*, 'IAPRS', Stuttgart, Germany, Vol. 32/4, pp. 527-532.

Shen J., Liu, X., Lu, G., and Zhou, w., 2002. Digital Photogrammetry and Cybercity Construction. *IAPRS, Commission II, Symposium 2002,* Vol. XXXIV, Part 2, Xi'an, P. R. China, Aug.20-23, 2002. pp. 413-416.

Scott, C., 2002. *Are all Orthos Created Equal? A Discussion of Orthophoto Accuracy,* [online]. Sanborn Product Manager. Available at: <URL: http://gis.csri.com/library/userconf/proc02/pap0265/p0265.htm > [Accessed 17 May 2007].

Steinbach, A., 1994. Working with GPS/INS. *The International Archives of the Photogrammetry, Remote Sensing and Spatial Information Sciences, Commission I,* WG I/5, Vol. 34, Part XXX-1, Sept.12-16, Como, Italy, 6 p, [online]. Available at: <URL: http://www.hansaluftbild.de> [Accessed 8 August 2008].

Shahin, F., 1994. A Hierarchical Approach for Digital Image Compression. *ASPRS/ACSM,* pp. 570-578.

Takagi, M., 1998. Accuraccy of Digital Elevation Model According to Spatial Resolution. In: D. Fritsch, M. Englich, and M. Sester, ed. *ISPRS commission IV symposium on GIS-Between versions and applications, IAPRS'* Stuttgart, Germany, Vol. 32/4, [online]. Available at :< URL: http://www.ifp.uni-stuttgart.de/publications/commIV/Takagi125.pdf>[Accessed 21 June 2007].

U.S. Department of the Interior, 1996. National Mapping Program Technical Instructions. Part 2: Standards for Digital Orthophotos, [online]. Available at :< http://rockyweb.cr.usgs.gov/nmpstds/acrodocs/doq/2DOQ1296.PDF> [Accessed 1 February 2007].

Walker, A. S., 1997. Practical Automation in Commercial Digital Photogrammetry. *Photogrammetric Records*, Vol. 15(89), pp. 657-664.

Wang, Y., Yang, X., M., Stojic, M., and Skelton B., 2002. A New Digital Photogrammetric System for GIS Professionals. *IAPRS*, Vol. XXXIV, Part 2, commission II, Xi'an, Aug.20-23, 2002, pp. 517-524.

Wolf, P. R., 1983. *Elements of Photogrammetry with Air Photo Interpretation and Remote Sensing*. 2nd ed. Wisconsin New York: McGraw-Hill, pp. 2-18.

Yamano, H., Shimazaki, H., Murase, T., Shigeki Sano, K., Suzuki, Y., Leenders, N., Forstreuter, W., and Kayanne, H., 2005. *Construction of Digital Elevation Models for Atoll Islands Using Digital Photogrammetry*, [online]. Available at: <URL: http://www.coastgis.org/cgis06/Papers/Yamano_DEM.pdf> [Accessed 20 May 2008].

Zhang, B., Fan, D., Guo, H., and Mao, T., 2002. Quantity Control of Digital Map. *Commission II, IAPRS*, Vol. XXXIV, Part 2, Xi'an, P. R. China, Aug.20-23, 2002. pp. 577-580.

Zhang, J., 2002. *A Comparison of Digital Photogrammetry and LIDAR high resolution digital elevation models.* Master Thesis, Geology and Geography, The Eberly College of Arts and Sciences, West Virginia University, Morgantown, West Virginia.

Zhang, J., and Sun, J., 2002. The Survey of Accuracy Analysis of Remote Sensing and GIS. *IAPRS, Commission II,* Vol. XXXIV, Part 2, Xi'an, P. R. China, Aug.20-23, 2002. pp. 581-584

Zhang, X., and Yuan, X., 2008. In: Wan, Y. et al., ed. *Proceedings of the 8th International Symposium on Spatial Accuracy Assessment in Natural Resources and Environmental Sciences.* Shanghai, P. R. China, June 25-27, 2008, World Academic Union (Press), pp. 30-36

APPENDICES

Appendix 1: An example of a DPS

Source: Geosystems

Appendix 2: Aerial Photography Film Report

AERIAL PHOTOGRAPHY FILM REPORT

Scale: 1:10,000		Colour Film Photography				Ghana LAP Orthophoto Project	
Camera Type	Serial No	F.Length	Filter	Magazine numbers		Film	
Leica RC 30	13215	152.86 mm	420 mm	4262/3871		Kodak Aerocolor III 2444	

Date		26/04/08		26/04/08		01/05/08	
Take off time		09:40		11:04		08:11:00	
Landing time		11:50		12:10		09:46:00	
Total hours		02:10		01:06		01:35	

Block Name	Date	Run	Dir	Altitude	Exposure Nos		Remarks
Goaso 7	26/04/08	1	270	5800ft	2471	2492	
Konongo 1	28/04/08	9	90	5800ft	2494	2513	
		8	270		2514	2533	
		7	90		2534	2553	
Kumasi 2	01/05/08	15/1	90	6000ft	2556	2585	East part west done 21/03
		16/1	270		2586	2647	
		16	90		2648	2688	Reflight part of the run
		17	270		2689	2726	38 frames western
							3 blanks + 20 tests

Navigator	Jussi-Pekka Saari	Remarks	Film Number
Pilot	James Bryan	01/05 partly under high cloud	6
Aircraft	G-BBTJ		

Appendix 3a: Camera Calibration Certificate

swissoptic
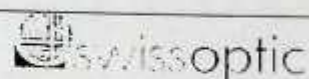
Camera Calibration Certificate

Object

Aerial Survey Camera Type	Lens Cone Type	Lens Serial No.	Remarks
RC 30	15/4 UAG-S	13215	

Acceptance

Characteristics	Acceptance	Remarks
Radial distortion	yes	
Photographic resolution	yes	
Principal point of autocollimation (PPA)	yes	
Principal point of symmetry (PPS)	yes	
Fiducial marks	yes	
Mean radial distortion	yes	
Radial distortion for semi-diagonals referred to PPS	yes	

Inspection

		Signature - Remarks
Date of calibration	10.09.2007	Lens cone operating hours
Inspector Name	Dietsche Paul	
Function	Supervisor	Signature
Inspection-No	SO 112	
Inspection plan Identification No.	187877	
Version	14.04.1989	
Lens cone calibration No.	870105	
Process specification Version	24.07.2006	

Maintenance

The last date, when service or overhaul of this lens cone was performed	02.10.2002	Lens cone operating hours	1180
Overhaul urgently required?	no	To avoid any malfunctions / damages it is recommended to perform a complete service / overhaul as soon as possible. See "Lens calibration process specification" of "RC 30 Technical Reference Manual".	

This Camera Calibration Certificate contains five pages. It may not be reproduced other than in full. Camera Calibration Certificates without signature and seal are not valid.

Appendix 3b

swissoptic
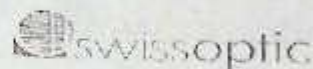
RC30   15/4 UAG-S   No. 13715   10.09.2007

Calibrated Focal Length (CFL)

Aperture	4
Filter on goniometer	VIS (400 - 700 nm)
Filter on camera	
C.F.L. :	152.86 mm

Radial distortion [micrometers]

Referred to principal point of symmetry (PPS)
Positive values denote image displacement away from center

Radius [mm]	Half - Sides				Mean
	1	2	3	4	
10	0.5	0.4	0.2	0.1	0.0
20	0.3	0.5	0.4	0.0	0.0
30	0.2	0.7	0.8	-0.4	0.0
40	0.1	0.6	0.4	0.1	0.1
50	0.0	1.1	0.2	0.5	0.2
60	-0.6	1.1	1.0	0.6	0.3
70	0.1	1.2	0.6	0.3	0.2
80	0.3	0.6	0.5	0.3	0.1
90	1.7	0.1	1.4	0.6	0.2
100	2.1	0.6	1.9	1.2	1.2
110	2.8	1.1	2.9	1.9	1.1
120	2.9	1.5	1.5	1.6	1.2
130	1.1	1.9	0.0	0.3	0.6
140	-2.6	0.1	3.5	-2.5	-2.0
148	-1.7	-2.1	-4.2	-3.3	-3.5

Photographic resolution [line pairs per millimeter]

Internal 3-line test chart contrast log 2.0

Aperture:	4.0
Filter:	VIS(400-700nm)
Film:	KODAK PANATOMIC X 2412
Developer:	KODAK HC110

Angle: [deg]	0	5	10	15	20	25	30	35	40	45
Radial	104	104	115	113	93	96	101	104	101	93
Tangential	117	116	114	109	87	56	76	79	72	56

AWAR (Area Weighted Average Resolution) in lp/mm   93

Seite7 (5)

Appendix 3c

swissoptic
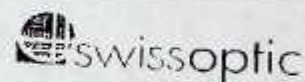
RC30   15/4 UAG-S   No.13215   19.09.2007

Principal point of autocollimation (PPA)
Principal point of symmetry (PPS)
Referred to central cross (FC), see diagram

	x[mm]	y[mm]
PPA	0.000	0.020
PPS	-0.007	0.017

Fiducial marks
Referred to central cross (FC)

	x[mm]	y[mm]
1	106.005	-106.003
2	-106.003	-106.000
3	-106.001	106.000
4	106.004	106.000

	x[mm]	y[mm]
5	0.003	-109.998
6	-110.003	-0.002
7	0.003	109.997
8	110.005	0.000
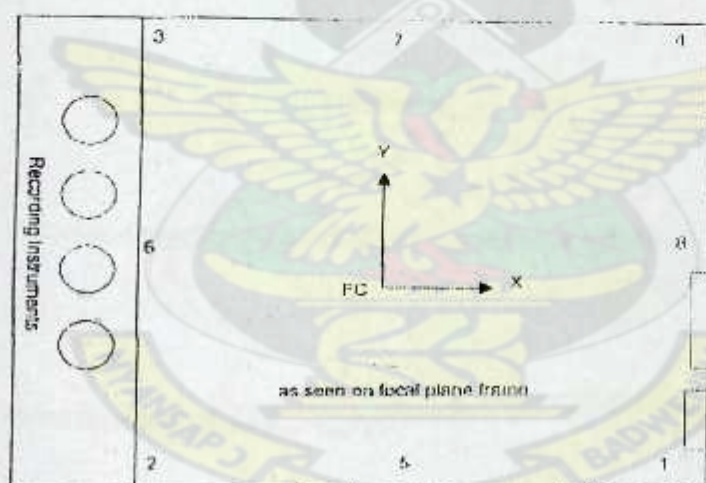
Seite3 (5)

56

Appendix 3d

| RC30 | 15/4 UAG-S | No. 13215 | swissoptic |
| 10.09.2007 |

Aperture:	4.0
Filter on goniometer	VIS (400 - 700 nm)
Filter on camera	--
C.F.L. :	152.86 mm

Mean radial distortion

Radial distortion for semi-diagonals referred to PPS

—□—1   —□—3   —■—2   -□-4

Serie 4 (5)

57

Appendix 3e

| RC30 | 15/4 UAG-S | No. 13215 | swissoptic |
| | | | 10.09.2007 |

Aperture	4.0
Filter on goniometer	VIS (400 - 700 nm)
Filter on camera	--
C.F.L.	152.86 mm

Mean radial distortion

Radial distortion for semi-diagonals referred to PPS

Seite 5 (5)
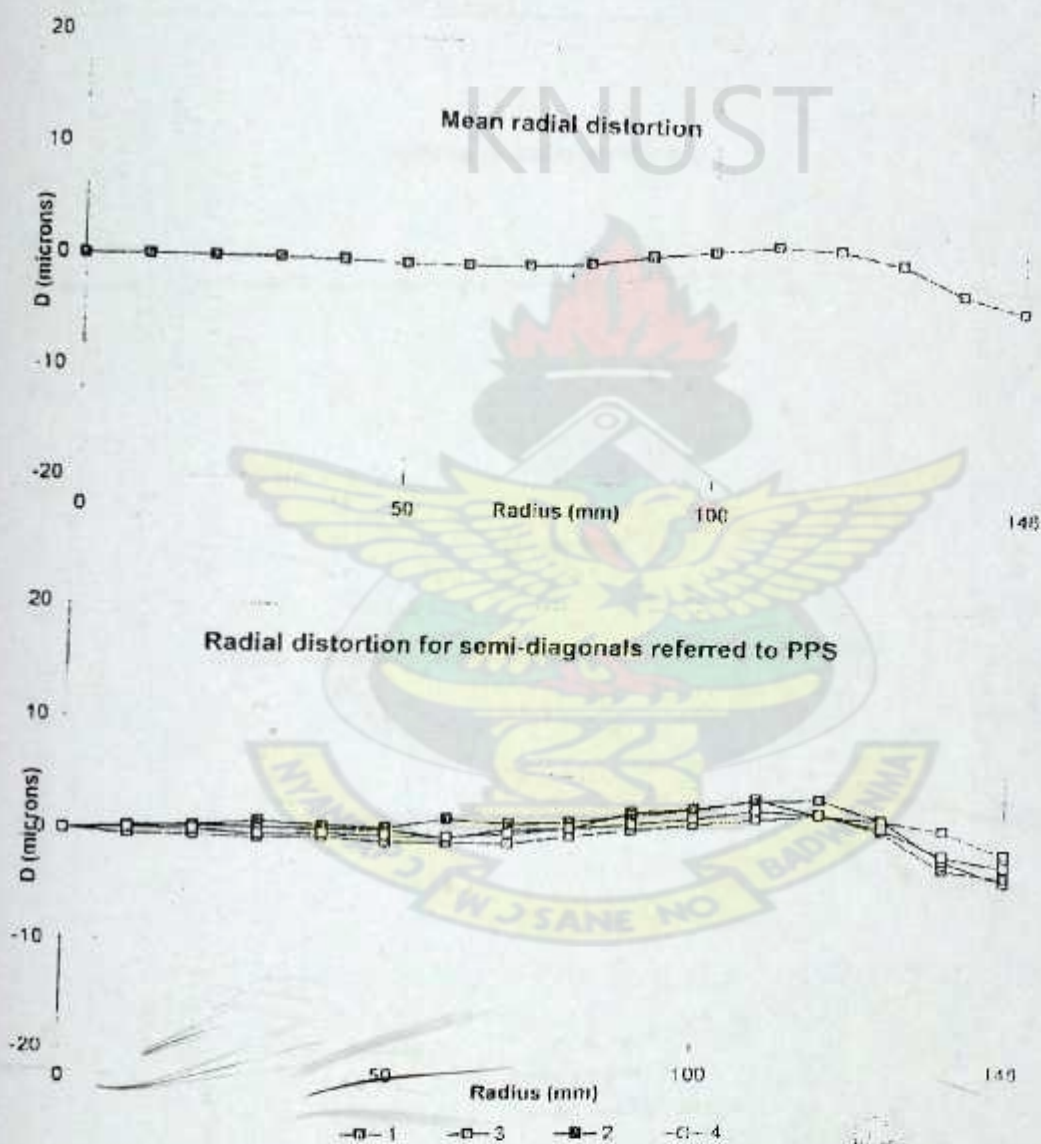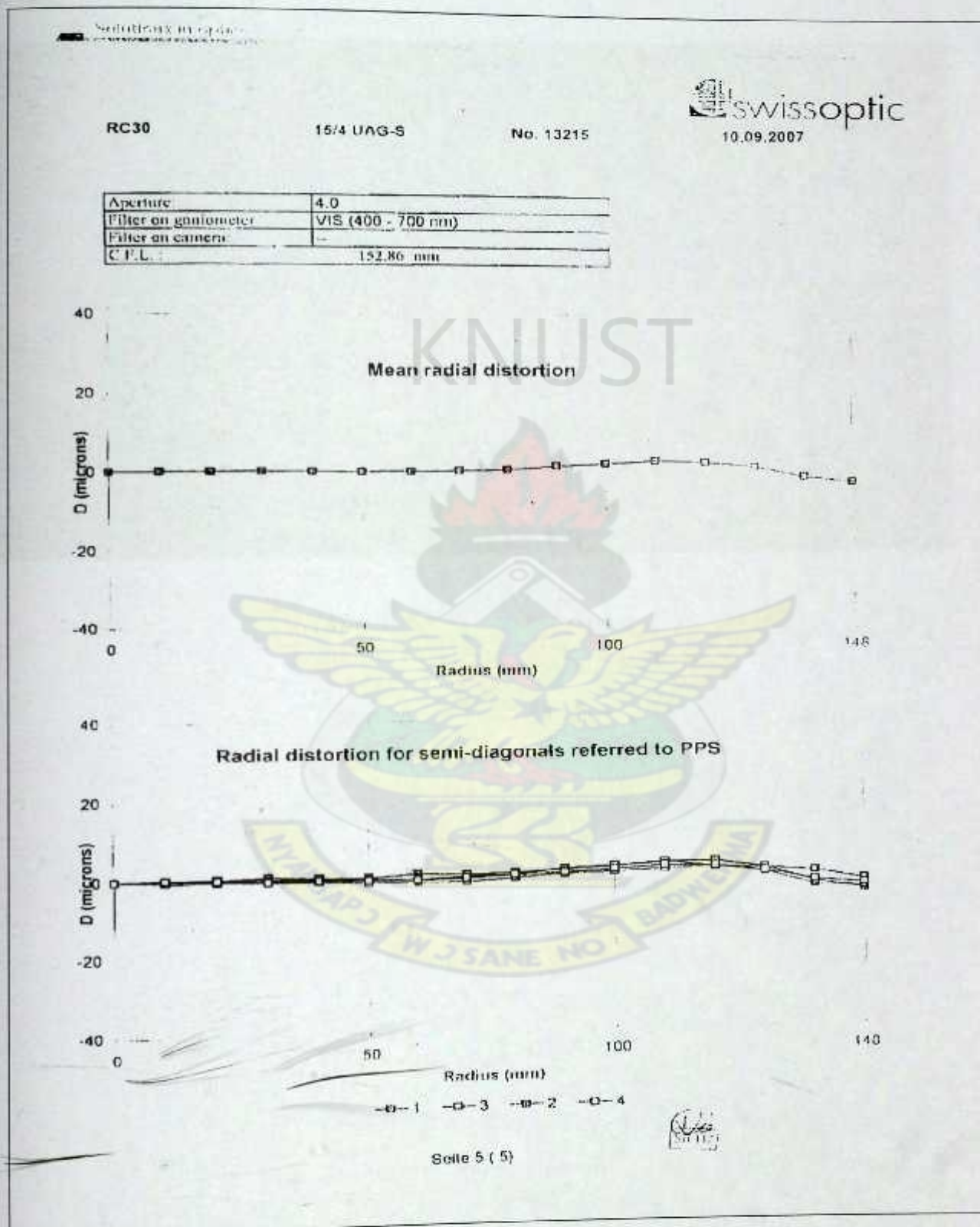
Appendix 4: Sample of GCP Station selection

Appendix 5: Recordings from the field observations of GCPs

Station ID	Device ID	Height of instrument (m)	Start Time (GMT)	End Time (GMT)
Observations for GCPs for Orientations				
SGA13/07/12	0003	1.233	9:18,12:30,16:56	12:27,16:45,17:35
GCP1	0001	1.618	9:36	9:57
A(CP13)	0001	1.587	10:18	10:38
GCP5	0001	1.488	11:30	11:50
GCP6	0001	1.476	11:58	12:18
GCP2	0001	1.482	12:27	12:47
GCP3(CP14)	0001	1.467	13:02	13:22
GCP4	0001	1.547	13:40	14:00
GCP12	0001	1.431	14:16	14:36
GCP8	0001	1.692	14:46	15:06
GCP7	0001	1.699	15:16	15:36
GCP11	0001	1.700	15:45	16:05
GCP10	0001	1.707	16:22	16:42
GCP9	0001	1.680	17:05	17:25
Field Observations for Check points				
SGA13/07/12	0003	1.286	8:21	16:43
CP1	0001	1.032	8:44	9:01
CP2	0001	1.268	9:26	9:45
CP3	0001	1.422	10:00	10:20
CP4	0001	1.617	10:35	10:55
CP12	0001	0.193	11:06	11:26
CP8	0001	0.193	11:40	12:00
CP7	0001	1.506	12:10	12:30
CP11	0001	0.193	12:38	12:58
CP6	0001	0.193	13:14	13:34
CP10	0001	0.193	13:43	14:03
CP9	0001	0.193	14:16	14:36
CP5	0001	0.193	14:44	15:04

Appendix 6a: Sample of GCP processing summary

Spectrum® Survey 3.50   PROCESS SUMMARY

Project: C:\...\Common\Spectrum Projects\MScSTUDENT PROJECT.spr

Coordinate System: UTM [Universal Transverse ...] Datum: WGS84
Geoid Model: Fixed [0.000m]   Units: Meters
Processing Date: 2008/09/10 19:09:27.79 (UTC)

VECTORS [13 total]

ALL VECTORS ARE FIXED

Vector/Occ.		Solution	Length	Used	Ratio	RMS	SD
GCP1-SGA	01	Fixed (L5 narrowlane)	464.317	99.73%	11.7	0.005	0.007
A-SGA	01	Fixed (L5 narrowlane)	1258.424	98.61%	4.7	0.005	0.008
GCP5-SGA	01	Fixed (L5 narrowlane)	121.761	95.53%	14.2	0.003	0.008
GCP6-SGA	01	Fixed (L5 narrowlane)	557.206	83.72%	7.0	0.007	0.011
GCP2-SGA	01	Fixed (L5 narrowlane)	700.769	85.59%	18.9	0.008	0.010
GCP3-SGA	01	Fixed (L5 narrowlane)	1137.744	64.20%	7.8	0.007	0.008
GCP11-SGA	01	Fixed (L5 narrowlane)	1042.281	92.17%	6.6	0.005	0.009
GCP10-SGA	01	Fixed (L5 narrowlane)	620.648	88.45%	4.4	0.006	0.009
GCP4-SGA	01	Fixed (L5 narrowlane)	1663.116	69.54%	7.0	0.008	0.010
GCP12-SGA	01	Fixed (L5 narrowlane)	1597.234	83.23%	8.2	0.005	0.011
GCP8-SGA	01	Fixed (L5 narrowlane)	1546.362	83.71%	4.3	0.005	0.008
GCP7-SGA	01	Fixed (L5 narrowlane)	1057.579	84.79%	5.2	0.005	0.009
GCP9-SGA	01	Fixed (L5 narrowlane)	409.502	88.83%	4.7	0.005	0.008

Appendix 6b RMS of GCPs used in study

GPS points	RMS(m)
GCP for orientation of DOIs	
GCP1	0.005
GCP2	0.008
GCP3(CP14)	0.007
GCP4	0.008
GCP5	0.003
GCP6	0.007
GCP7	0.005
GCP8	0.005
GCP9	0.005
GCP10	0.006
GCP11	0.005
GCP12	0.005
Checkpoints for accuracy analysis	
CP1	0.004
CP2	0.006
CP3	0.008
CP4	0.003
CP5	0.005
CP6	0.004
CP7	0.006
CP8	0.007
CP9	0.006
CP10	0.005
CP11	0.006
CP12	0.005
CP13	0.005

Appendix 7: GCPs Used in the study

Point Name	Eastern(m)	Northern(m)	Height(m)
GCPs for DOI orientation			
SGA 13/07/12	659601.749	739698.498	277.692
GCP1	660056.915	739788.940	264.294
GCP2	660023.155	740258.292	278.328
GCP3(CP14)	660065.176	740737.409	283.144
GCP4	660081.652	741290.641	272.516
GCP5	659652.121	739809.333	277.850
GCP6	659638.866	740254.332	269.331
GCP7	659754.971	740744.754	269.981
GCP8	659783.830	741233.896	282.237
GCP9	659201.108	739782.191	266.223
GCP10	659240.304	740202.512	256.888
GCP11	659450.167	740729.535	270.179
GCP12	659209.038	741246.358	257.385
GCPs for accuracy analysis			
CP1	659996.484	739758.853	264.026
CP2	660010.462	740212.048	277.030
CP3	660147.499	740692.320	284.072
CP4	660003.428	741265.428	275.518
CP5	659575.588	739844.412	276.313
CP6	659632.450	740248.492	271.161
CP7	659756.853	740749.666	270.298
CP8	659785.667	741177.144	278.227
CP9	659222.600	739744.291	269.286
CP10	659248.885	740278.882	255.000
CP11	659463.953	740738.146	270.113
CP12	659413.800	741255.619	263.390
CP13	660078.119	740863.085	283.544

Appendix 8: RMS for IO

Date: 08:11:57 11/09/2008

Images: 2561 and 2562

Type: Automatic IO (used time 1 second(s))

RMS computation for Image 2561 and 2562

Transformation parameters used	Image 2561	Image 2562
	6 Parameter (2 rot., 2 scale)	6 Parameter (2 rot., 2 scale)
Origin[mm]	-126.7204, 119.0663	-126.9914 118.9492
Scale	0.0200 0.0200	0.0200 0.0200
Rotation Axes[grad]	0.0941 -199.9031	0.1453 -199.8516
Sigma0 [mm]	0.0084	0.0070
r.m.s. [mm]	0.0033	0.0028

Appendix 9: A summary of AT statistics results

No. of GCPs	mean standard deviation ground(m)			R.M.S for terrain control(m)			mean standard deviation of orientation (deg/1000)			Sigma0(μ) Of DOI
	X	Y	Z	X	Y	Z	Omega	Phi	kapa	
10GCPs	0.043	0.054	0.110	0.005	0.007	0.023	4.7	7.4	1.9	4.4
7GCPs	0.062	0.075	0.156	0.012	0.017	0.024	6.7	9.7	2.7	5.7
4GCPs	0.075	0.091	0.180	0.030	0.007	0.030	7.9	10.9	3.0	6.2

Appendix 10: RMSE of Georeferencing of DOI from edited DEM

Link Table

Link	X Source	Y Source	X Map	Y Map	Residual
1	660065.066093	740737.958357	699756.742000	736356.028000	0.75652
2	659208.978589	741247.409079	696954.446000	738036.569000	0.13105
3	659203.112495	739780.882672	696908.545000	733233.246000	0.65461
4	660023.577957	740257.831802	699612.206000	734784.451000	0.52735
5	660057.865114	739787.604098	699715.848000	733244.874000	0.52745
6	659450.551208	740729.581571	697738.825000	736338.175000	0.71159
7	659783.100241	741234.806068	698839.342000	737987.817000	0.32089
8	659653.514448	739808.069069	698388.852000	733317.188000	0.47325
9	660080.764024	741291.842092	699818.215000	738170.824000	0.24856
10	659639.694938	740253.882185	698351.103000	734777.261000	0.18039
11	659755.103624	740745.026916	698738.944000	736384.031000	0.04017

☑ Auto Adjust   Transformation: 1st Order Polynomial (AI ▼)   Total RMS Error: 0.47707

Load...   Save...   Restore From Dataset   OK

Appendix 11: Computed RMSE, and accuracy, of DOIs from discrepancies

Appendix 11a:10 GCP DOI

	Checkpoints WGS 84		DOI coordinates WGS 84		Discrepancies		Squared Discrepancies	
Point	Easting(Y)	Northing(X)	Easting(Y)	Northing(X)	ΔY	ΔX	ΔY^2	ΔX^2
GCP1	659996.484	739758.853	659997.270	739759.179	0.786	0.326	0.618	0.106
GCP2	660010.462	740212.048	660011.115	740212.063	0.653	0.015	0.426	0.000
GCP3	660147.499	740692.320	660147.713	740692.088	0.214	-0.232	0.046	0.054
GCP4	660003.428	741265.428	660003.041	741264.886	-0.387	-0.542	0.150	0.294
GCP5	659575.588	739844.412	659576.787	739843.480	1.199	-0.932	1.438	0.869
GCP6	659632.450	740248.492	659633.738	740247.894	1.288	-0.598	1.659	0.358
GCP7	659756.853	740749.666	659756.953	740749.385	0.100	-0.281	0.010	0.079
GCP8	659785.667	741177.144	659785.760	741176.571	0.093	-0.573	0.009	0.328
GCP9	659222.600	739744.291	659223.962	739744.349	1.362	0.058	1.855	0.003
GCP10	659248.885	740278.882	659249.923	740278.109	1.038	-0.773	1.077	0.598
GCP11	659463.953	740738.146	659464.675	740737.277	0.722	-0.869	0.521	0.755
GCP12	659413.800	741255.619	659413.882	741255.345	0.082	-0.274	0.007	0.075
GCP13	660078.119	740863.085	660079.663	740860.686	1.544	-2.399	2.384	5.755
GCP14	659601.749	739698.498	659602.864	739698.657	1.115	0.159	1.243	0.025
						Sums	11.443	9.299
						MSE	0.817	0.664
						RMSExy(σxy)	0.904	0.815
						RMSEr		1.217
						Accuracy,(m)		2.104

Computation of RMSE, and Accuracy, from discrepancies

67

Appendix 11b:7 GCP DOI

Point	Checkpoints WGS 84		Measured DOP coordinates WGS 84		DOP coordinates minus checkpoints		Discrepancies squared as required for RMSE	
	Easting(Y)	Northing(X)	Easting(Y)	Northing(X)	ΔY	ΔX	ΔY^2	ΔX^2
GCP1	659996.484	739758.853	659997.748	739759.166	1.264	0.313	1.598	0.098
GCP2	660010.462	740212.048	660011.445	740212.226	0.983	0.178	0.966	0.032
GCP3	660147.499	740692.320	660148.069	740692.198	0.57	-0.122	0.325	0.015
GCP4	660003.428	741265.428	660003.099	741264.648	-0.329	-0.78	0.108	0.608
GCP5	659575.588	739844.412	659577.217	739843.480	1.629	-0.932	2.654	0.869
GCP6	659632.450	740248.492	659634.242	740247.897	1.792	-0.595	3.211	0.354
GCP7	659756.853	740749.666	659757.211	740749.446	0.358	-0.22	0.128	0.048
GCP8	659785.667	741177.144	659786.008	741176.677	0.341	-0.467	0.116	0.218
GCP9	659222.600	739744.291	659224.662	739743.805	2.062	-0.486	4.252	0.236
GCP10	659248.885	740278.882	659250.267	740277.857	1.382	-1.025	1.910	1.051
GCP11	659463.953	740738.146	659465.054	740737.202	1.101	-0.944	1.212	0.891
GCP12	659413.800	741255.619	659414.324	741255.141	0.524	-0.478	0.275	0.228
GCP13	660078.119	740863.085	660080.174	740860.925	2.055	-2.16	4.223	4.666
GCP14	659601.749	739698.498	659603.399	739698.610	1.65	0.112	2.723	0.013
						Sums	23.701	9.327
						MSE	1.693	0.666
						RMSExy(oxy)	1.301	0.816
						RMSEr		1.536
						Accuracy_r(m)		2.591

Computation of $RMSE_r$ and $Accuracy_r$ from discrepancies

68

Appendix 11c:4 GCP DOI

Point	Checkpoints WGS 84		Measured DOP coordinates WGS 84		DOP coordinates minus checkpoints		Discrepancies squared as required for RMSE	
	Easting(Y)	Northing(X)	Easting(Y)	Northing(X)	ΔY	ΔX	ΔY^2	ΔX^2
GCP1	659996.484	739758.853	659997.375	739758.011	0.891	-0.842	0.794	0.709
GCP2	660010.462	740212.048	660011.267	740211.271	0.805	-0.777	0.648	0.604
GCP3	660147.499	740692.320	660148.039	740691.500	0.54	-0.820	0.292	0.672
GCP4	660003.428	741265.428	660003.310	741264.052	-0.118	-1.376	0.014	1.893
GCP5	659575.588	739844.412	659576.185	739843.819	0.597	-0.593	0.356	0.352
GCP6	659632.450	740248.492	659633.892	740246.92	1.442	-1.572	2.079	2.471
GCP7	659756.853	740749.666	659757.147	740748.714	0.294	-0.952	0.086	0.906
GCP8	659785.667	741177.144	659785.953	741176.07	0.286	-1.074	0.082	1.153
GCP9	659222.600	739744.291	659223.943	739742.715	1.343	-1.576	1.804	2.484
GCP10	659248.885	740278.882	659249.796	740277.068	0.911	-1.814	0.830	3.291
GCP11	659463.953	740738.146	659464.751	740736.469	0.798	-1.677	0.637	2.812
GCP12	659413.800	741255.619	659414.247	741254.835	0.447	-0.784	0.200	0.615
GCP13	660078.119	740863.085	660080.338	740859.932	2.219	-3.153	4.924	9.941
GCP14	659601.749	739698.498	659602.863	739697.663	1.114	-0.835	1.241	0.697
						Sums	13.987	28.601
						MSE	0.999	2.043
						RMSExy(oxy)	1.000	1.429
						RMSEr		1.744
						Accuracyr(m)		2.973

Computation of RMSE$_r$ and Accuracy$_r$ from discrepancies

69

Appendix 11d: 9m DTM grid interval DOI

Point	Checkpoints WGS 84		Measured DOP coordinates WGS 84		DOP coordinates minus checkpoints		Discrepancies squared as required for RMSE	
	Easting(Y)	Northing(X)	Easting(Y)	Northing(X)	ΔY	ΔX	ΔY^2	ΔX^2
GCP1	659996.484	739758.853	659997.306	739759.055	0.822	0.202	0.676	0.041
GCP2	660010.462	740212.048	660011.040	740212.045	0.578	-0.003	0.334	0.000
GCP3	660147.499	740692.320	660147.709	740692.277	0.210	-0.043	0.044	0.002
GCP4	660003.428	741265.428	660003.076	741264.956	-0.352	-0.472	0.124	0.223
GCP5	659575.588	739844.412	659576.771	739843.439	1.183	-0.973	1.399	0.947
GCP6	659632.450	740248.492	659633.836	740247.838	1.386	-0.654	1.921	0.428
GCP7	659756.853	740749.666	659757.145	740749.440	0.292	-0.226	0.085	0.051
GCP8	659785.667	741177.144	659785.024	741177.183	-0.643	0.039	0.413	0.002
GCP9	659222.600	739744.291	659224.045	739744.478	1.445	0.187	2.088	0.035
GCP10	659248.885	740278.882	659249.847	740278.092	0.962	-0.79	0.925	0.624
GCP11	659463.953	740738.146	659464.719	740737.199	0.766	-0.947	0.587	0.897
GCP12	659413.800	741255.619	659413.818	741255.624	0.018	0.005	0.000	0.000
GCP13	660078.119	740863.085	660079.905	740860.796	1.786	-2.289	3.90	5.240
GCP14	659601.749	739698.498	659602.959	739698.609	1.210	0.111	1.464	0.012
						Sums	13.251	8.500
						MSE	0.947	0.607
						RMSExy(σxy)	0.973	0.779
						RMSEr		1.246
						Accuracyr(m)		2.144

Computation of RMSEr and Accuracyr from discrepancies

70

Appendix 11e: 12m DTM grid interval DOI

Point	Checkpoints WGS 84		Measured DOP coordinates WGS 84		DOP coordinates minus checkpoints		Discrepancies squared as required for RMSE	
	Easting(Y)	Northing(X)	Easting(Y)	Northing(X)	ΔY	ΔX	ΔY^2	ΔX^2
GCP1	659996.484	739758.853	659997.338	739759.142	0.854	0.289	0.729	0.084
GCP2	660010.462	740212.048	660011.114	740212.084	0.652	0.036	0.425	0.001
GCP3	660147.499	740692.320	660147.962	740692.195	0.463	-0.125	0.214	0.016
GCP4	660003.428	741265.428	660003.312	741264.811	-0.116	-0.617	0.013	0.381
GCP5	659575.588	739844.412	659576.709	739843.640	1.121	-0.772	1.257	0.596
GCP6	659632.450	740248.492	659633.683	740247.680	1.233	-0.812	1.520	0.659
GCP7	659756.853	740749.666	659757.190	740749.464	0.337	-0.202	0.114	0.041
GCP8	659785.667	741177.144	659785.001	741177.084	-0.666	-0.06	0.444	0.004
GCP9	659222.600	739744.291	659224.096	739744.247	1.496	-0.044	2.238	0.002
GCP10	659248.885	740278.882	659249.812	740278.151	0.927	-0.731	0.859	0.534
GCP11	659463.953	740738.146	659464.692	740737.137	0.739	-1.009	0.546	1.018
GCP12	659413.800	741255.619	659414.170	741255.294	0.37	-0.325	0.137	0.106
GCP13	660078.119	740863.085	660079.957	740860.659	1.838	-2.426	3.378	5.885
GCP14	659601.749	739698.498	659602.999	739698.608	1.250	0.110	1.563	0.012
						Sums	13.437	9.338
						MSE	0.960	0.667
						RMSExy(oxy)	0.980	0.817
						RMSEr		1.275
						Accuracyr(m)		2.199

Computation of RMSEr and Accuracyr from discrepancies

71

Appendix 11f: 50m DTM grid interval DOI

Point	Checkpoints WGS 84		Measured DOP coordinates WGS 84		DOP coordinates minus checkpoints		Discrepancies squared as required for RMSE	
	Easting(Y)	Northing(X)	Easting(Y)	Northing(X)	ΔY	ΔX	ΔY^2	ΔX^2
GCP1	659996.484	739758.853	659997.439	739759.287	0.955	0.434	0.912	0.188
GCP2	660010.462	740212.048	660011.115	740212.050	0.653	0.002	0.426	0.000
GCP3	660147.499	740692.320	660147.966	740692.247	0.467	-0.073	0.218	0.005
GCP4	660003.428	741265.428	660003.327	741263.999	-0.101	-1.429	0.010	2.042
GCP5	659575.588	739844.412	659576.343	739844.539	0.755	0.127	0.570	0.016
GCP6	659632.450	740248.492	659633.376	740247.909	0.926	-0.583	0.857	0.340
GCP7	659756.853	740749.666	659756.844	740749.506	-0.009	-0.16	0.000	0.026
GCP8	659785.667	741177.144	659784.980	741177.279	-0.687	0.135	0.472	0.018
GCP9	659222.600	739744.291	659224.045	739743.869	1.445	-0.422	2.088	0.178
GCP10	659248.885	740278.882	659249.892	740278.139	1.007	-0.743	1.014	0.552
GCP11	659463.953	740738.146	659464.716	740737.178	0.763	-0.968	0.582	0.937
GCP12	659413.800	741255.619	659414.066	741255.672	0.266	0.053	0.071	0.003
GCP13	660078.119	740863.085	660079.920	740860.610	1.801	-2.475	3.244	6.126
GCP14	659601.749	739698.498	659602.994	739699.198	1.245	0.7	1.550	0.490
						Sums	12.015	10.921
						MSE	0.858	0.780
						RMSExy(σxy)	0.926	
						RMSEr	1.280	
						Accuracyr(m)	2.215	

Computation of RMSEr and Accuracyr from discrepancies

72

Appendix 11g: 1:2,500 scale DOI

Point	Checkpoints WGS 84		Measured DOP coordinates WGS 84		DOP coordinates minus checkpoints		Discrepancies squared as required for RMSE	
	Easting(Y)	Northing(X)	Easting(Y)	Northing(X)	ΔY	ΔX	ΔY^2	ΔX^2
GCP1	659996.484	739758.853	659997.492	739759.063	1.008	0.210	1.016	0.044
GCP2	660010.462	740212.048	660011.069	740212.113	0.607	0.065	0.368	0.004
GCP3	660147.499	740692.320	660147.933	740692.218	0.434	-0.102	0.188	0.010
GCP4	660003.428	741265.428	660003.337	741264.763	-0.091	-0.665	0.008	0.442
GCP5	659575.588	739844.412	659576.672	739843.614	1.084	-0.798	1.175	0.637
GCP6	659632.450	740248.492	659633.848	740247.733	1.398	-0.759	1.954	0.576
GCP7	659756.853	740749.666	659757.102	740749.177	0.249	-0.489	0.062	0.239
GCP8	659785.667	741177.144	659785.099	741177.223	-0.568	0.079	0.323	0.006
GCP9	659222.600	739744.291	659224.111	739744.304	1.511	0.013	2.283	0.000
GCP10	659248.885	740278.882	659249.804	740278.143	0.919	-0.739	0.845	0.546
GCP11	659463.953	740738.146	659464.733	740737.308	0.78	-0.838	0.608	0.702
GCP12	659413.800	741255.619	659414.17	741255.252	0.37	-0.367	0.137	0.135
GCP13	660078.119	740863.085	660079.835	740860.672	1.716	-2.413	2.945	5.823
GCP14	659601.749	739698.498	659603.006	739698.585	1.257	0.087	1.580	0.008
						Sums	13.493	9.173
						MSE	0.964	0.655
						RMSExy(σxy)	0.982	0.809
						RMSEr		1.272
						Accuracy,(m)		2.192

Compuation of RMSE, and Accuracy, from discrepancies

73

Appendix 11b: 1: 5,000 scale DOI

Point	Checkpoints WGS 84		Measured DOP coordinates WGS 84		DOP coordinates minus checkpoints		Discrepancies squared as required for RMSE	
	Easting(Y)	Northing(X)	Easting(Y)	Northing(X)	ΔY	ΔX	ΔY^2	ΔX^2
GCP1	659996.484	739758.853	6599997.398	739759.185	0.914	0.332	0.835	0.110
GCP2	660010.462	740212.048	660011.058	740212.118	0.596	0.070	0.355	0.005
GCP3	660147.499	740692.320	660147.865	740692.219	0.366	-0.101	0.134	0.010
GCP4	660003.428	741265.428	660003.098	741264.787	-0.33	-0.641	0.109	0.411
GCP5	659575.588	739844.412	659576.930	739843.477	1.342	-0.935	1.801	0.874
GCP6	659632.450	740248.492	659633.713	740247.800	1.263	-0.692	1.595	0.479
GCP7	659756.853	740749.666	659756.933	740749.240	0.08	-0.426	0.006	0.181
GCP8	659785.667	741177.144	659785.129	741177.186	-0.538	0.042	0.289	0.002
GCP9	659222.600	739744.291	659224.067	739744.186	1.467	-0.105	2.152	0.011
GCP10	659248.885	740278.882	659249.941	740278.055	1.056	-0.827	1.115	0.684
GCP11	659463.953	740738.146	659464.571	740737.315	0.618	-0.831	0.382	0.691
GCP12	659413.800	741255.619	659414.116	741255.333	0.316	-0.286	0.100	0.082
GCP13	660078.119	740863.085	660079.818	740860.542	1.699	-2.543	2.887	6.467
GCP14	659601.749	739698.498	659603.008	739698.677	1.259	0.179	1.585	0.032
						Sums	13.346	10.039
						MSE	0.953	0.717
						RMSExy(oxy)	0.976	0.847
						$RMSE_r$	1.292	
						$Accuracy_r(m)$	2.231	

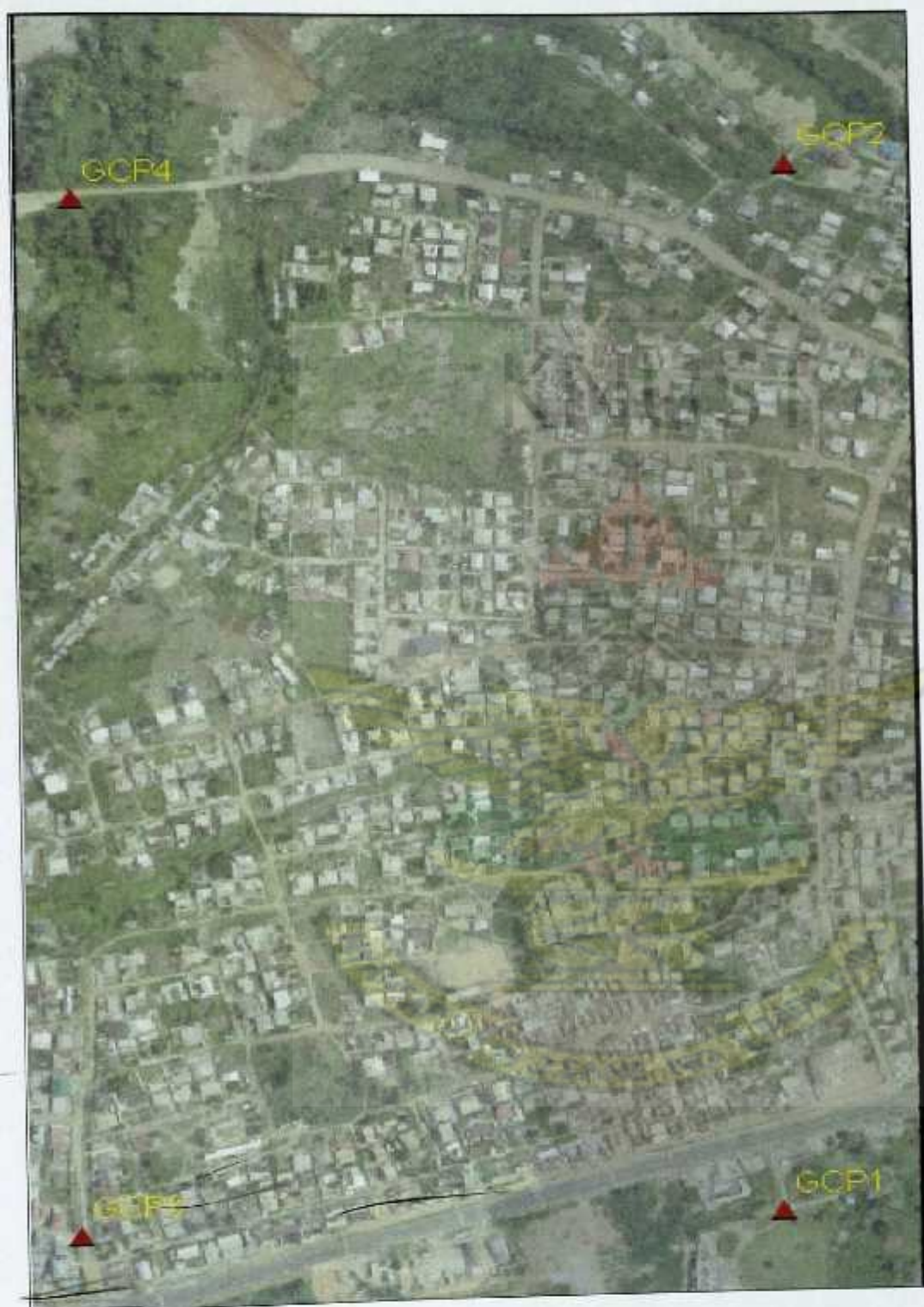Computation of $RMSE_r$ and $Accuracy_r$ from discrepancies

74

Appendix 11i: 1:10,000 scale DOI

Point	Checkpoints WGS 84		Measured DOP coordinates WGS 84		DOP coordinates minus checkpoints		Discrepancies squared as required for RMSE	
	Easting(Y)	Northing(X)	Easting(Y)	Northing(X)	ΔY	ΔX	ΔY^2	ΔX^2
GCP1	659996.484	739758.853	659997.372	739759.817	0.888	0.964	0.789	0.929
GCP2	660010.462	740212.048	660010.464	740211.815	0.002	-0.233	0.000	0.054
GCP3	660147.499	740692.320	660147.498	740692.431	-0.001	0.111	0.000	0.012
GCP4	660003.428	741265.428	660003.911	741265.530	0.483	0.102	0.233	0.010
GCP5	659575.588	739844.412	659576.522	739843.152	0.934	-1.26	0.872	1.588
GCP6	659632.450	740248.492	659634.046	740247.726	1.596	-0.766	2.547	0.587
GCP7	659756.853	740749.666	659756.998	740749.220	0.145	-0.446	0.021	0.199
GCP8	659785.667	741177.144	659784.590	741177.918	-1.077	0.774	1.160	0.599
GCP9	659222.600	739744.291	659224.038	739743.536	1.438	-0.755	2.068	0.570
GCP10	659248.885	740278.882	659249.971	740277.726	1.086	-1.156	1.179	1.336
GCP11	659463.953	740738.146	659465.006	740738.923	1.053	0.777	1.109	0.604
GCP12	659413.800	741255.619	659414.405	741256.626	0.605	1.007	0.366	1.014
GCP13	660078.119	740863.085	660079.149	740861.201	1.03	-1.884	1.061	3.549
GCP14	659601.749	739698.498	659602.994	739698.625	1.245	0.127	1.550	0.016
						Sums	12.955	11.068
						MSE	0.925	0.791
						RMSExy(σxy)	0.962	0.889
						RMSE_r		1.310
						Accuracy_r(m)		2.265

Computation of RMSE_r and Accuracy_r from discrepancies

Appendix 11j: Edited DEM DOI

Checkpoints WGS 84			DOI coordinates WGS 84		Discrepancies		Squared Discrepancies	
Point	Easting(Y)	Northing(X)	Easting(Y)	Northing(X)	ΔY	ΔX	ΔY^2	ΔX^2
GCP1	659996.484	739758.853	659997.027	739759.179	0.543	0.326	0.295	0.106
GCP2	660010.462	740212.048	660011.115	740212.063	0.653	0.015	0.426	0.000
GCP3	660147.499	740692.32	660147.713	740692.088	0.214	-0.232	0.046	0.054
GCP4	660003.428	741265.428	660003.041	741264.886	-0.387	-0.542	0.150	0.294
GCP5	659575.588	739844.412	659576.787	739843.48	1.199	-0.932	1.438	0.869
GCP6	659632.45	740248.492	659633.038	740247.894	0.588	-0.598	0.346	0.358
GCP7	659756.853	740749.666	659756.953	740749.385	0.100	-0.281	0.010	0.079
GCP8	659785.667	741177.144	659785.76	741176.571	0.093	-0.573	0.009	0.328
GCP9	659222.6	739744.291	659223.962	739744.349	1.362	0.058	1.855	0.003
GCP10	659248.885	740278.882	659249.223	740278.109	0.338	-0.773	0.114	0.598
GCP11	659463.953	740738.146	659464.675	740737.277	0.722	-0.869	0.521	0.755
GCP12	659413.8	741255.619	659413.882	741255.345	0.082	-0.274	0.007	0.075
GCP13	660078.119	740863.085	660079.063	740860.686	0.944	-2.399	0.891	5.755
GCP14	659601.749	739698.498	659602.864	739698.657	1.115	0.159	1.243	0.025
						Sums	7.350	9.299
						MSE	0.525	0.664
						RMSExy(σxy)	0.725	0.815
						RMSEr		1.091
						Accuracyr(m)		1.884

Computation of RMSEr and Accuracyr from discrepancies

76

Appendix 12a: Distribution of GCPs in DOIs (4GCP DOI)

Appendix 12b: 7 GCP DOI

Appendix 12c: 10 GCP DOI

Appendix 13: Correction of masspoints (left photo) with breaklines (right photo)